Design of a High Performance Liquid-cooled Lithium-ion Battery Pack for Automotive Applications

by

Ethan Perrin

Submitted to the

in partial fulfillment of the requirements for the degree of

Bachelor of Science in Mechanical Engineering

at the

MASSACHUSETTS INSTITUTE OF TECHNOLOGY

May 2020

Author . . . .
Department of Mechanical Engineering
May 08, 2020

Certified by. . . . .
Ian W. Hunter
George N. Hatsopoulos Professor in Thermodynamics
Thesis Supervisor

Accepted by . . . .
Maria Yang
Professor of Mechanical Engineering

Design of a High Performance Liquid-cooled Lithium-ion Battery Pack for Automotive Applications

by

Ethan Perrin

Abstract

This thesis explores the design of a water cooled lithium ion battery module for use in high power automotive applications such as an FSAE Electric racecar. The motivation for liquid cooling in this application is presented with an adiabatic battery heating simulation followed by a discussion of axial cooling based on the internal construction of an 18650 battery cell. A novel design is proposed, implementing soldering the negative terminal of electroplated 18650 battery cells directly to a metal core printed circuit board material as the critical cell-to-water interface that provides high thermal conductivity while maintaining electrical isolation. Cold plate design, sealing, and manufacturing is discussed and implemented concluding with pressure and leak testing of a scale test article. Cell soldering efficacy is explored through testing of various low temperature solder alloys, fluxes, and surface plating to make recommendations on full scale module builds. A single cell test article is constructed and tested to validate thermal performance expectations with preliminary results suggesting constant power discharge rates of up to 60 W per cell is possible without overheating, which greatly exceeds the power requirements of existing FSAE Electric vehicles built by MIT Motorsports. Further work is needed to quantify solder joint reliability and examine thermal gradients present at the full module and pack scales.

Thesis Supervisor: Ian W. Hunter
Title: George N. Hatsopoulos Professor in Thermodynamics

Acknowledgments

First and foremost, I would like to thank the Edgerton Center for supporting MIT Motorsports and making it possible for student teams to explore independently organized hands-on technical work outside of the traditional academic setting. Without the work space, funding, and administrative organization provided by the Edgerton Center staff, I would not have been able to spend the vast majority of my time in N51 and N52 exploring machining, electronics, and racecar building that is truly impossible to experience anywhere else on campus.

In particular, I would like to thank my team members Elliot Owen, Jeremy Noel, and Serena Grown-Haeberli for their consistent friendship, support, and engineering teamwork over the past four years. I owe a huge debt of gratitude to Asli Demir, for spending literally thousands of hours working with me at all hours of day to produce the finest FSAE battery packs on American asphalt. Without her meticulous attention to detail and incredible patience I would not be where I am today.

This research would also not be possible without several key sponsors – Indium Corporation for graciously providing indium research kits and technical consultation; Lucid Motors for supplying battery cells; and Tektronix for their excellent test equipment that makes testing and data collection an absolute pleasure. I would also like to thank Professor Ian Hunter, Dr. Cathy Hogan, Shibani Joshi, and all the researchers and students at the Bioinstrumentation lab for assistance and advising my thesis work as my final semester at MIT came to an unexpected conclusion amid a global health crisis.

Contents

List of Figures

1

Introduction

1.1 FSAE Electric Competition

The Society of Automotive Engineers (SAE) started the Formula SAE competition in 1981 as one of several events in the Collegiate Design Series competitions. Formula SAE challenges student teams to design, build, and compete with small F1 style vehicles evaluated in static and dynamic events to earn points based on engineering understanding and technical performance. In 2013, SAE introduced the Formula SAE Electric competition challenging students to design and build electric vehicles utilizing batteries as energy storage and electric motors for traction [1]. After competing for years in the standard gasoline engine competition, MIT's student team MIT Motorsports switched to the electric competition in 2013. Vehicles compete in dynamic events testing straight-line acceleration, cornering, autocross performance, endurance capability, and efficiency. The teams are also evaluated on the technical merit of their vehicle, the theoretical small-run production cost, and theoretical business model. In each event, teams are scored in a points-based system with the most points overall dictating the winning team. Dynamic driving events represent the largest fraction of the points and therefore motivate design of a vehicle with very high performance. The Endurance event entails a 22 km autocross race worth approximately 1/3 of the total points. Drivers must pilot the car through 16 laps as quickly as possible to post the best overall time to earn the most points, ideally pushing the vehicle to the

Figure 1-1: MY18 at the Formula SAE Electric 2018 Competition in Lincoln, Nebraska.

limits throughout. The duration, environment, and required vehicle performance in this event drives the functional requirements of the battery pack in terms of mass, energy, and power capability. Due to the autocross nature of the event, vehicles are repeatedly accelerating and decelerating at each and every corner, placing huge demand on the battery pack to deliver high peak power. The heat generated by the battery pack rises quickly under load due to the high power density of the system, and electric vehicles are frequently forced to limit power use when reaching the rules-imposed battery temperature limit of $60°C$. Vehicles in the Formula SAE Electric competition are subject to a highly detailed set of rules oriented at ensuring safety of the vehicles to be built and operated by student teams. This rule set imposes additional requirements on mechanical and electrical design that must be adhered to for safety and competition eligibility.

1.2   Prior Work - MY19

The Model Year 2019 vehicle was MIT Motorsports' first attempt at advancing powertrain technology to include a custom built liquid cooled battery pack and four-

wheel drive architecture, implementing a single inboard rear motor and dual outboard front motors with custom built planetary gearboxes. This design was aimed at producing a vehicle reaching peak acceleration performance in dynamic events by utilizing all four wheels for traction fueled by a liquid cooled battery to prevent overheating in the endurance event that imposes a performance limitation. Though significant technical leaps were made in development of the 2019 battery pack that served to deliver excellent cooling performance, the pack was ultimately unfit for competition due to electrical isolation issues and fluid leaks. The overall architecture of the battery pack was proven despite these flaws, and carried over into development of further designs that hope to improve on isolation and sealing issues.

Figure 1-2: MY19 at the Formula SAE Electric 2019 Competition in Lincoln, Nebraska.

1.3   Thesis Scope

The engineering goal is to develop a battery cooling technology that abides by the competition rule set and allows the vehicle to perform unhindered by thermal

17

limitations of the battery cells in the 22 km endurance event. Research into battery cell selection, cell performance evaluation, pack modeling sizing, battery monitoring systems, and performance simulation are not included in the scope of this work.

2

Battery Design Background

Vehicles in the Formula SAE Electric competition almost universally utilize cylindrical lithium-ion or pouch lithium-polymer battery cells for their high energy density, high power capability, and wide commercial availability due to integration in consumer products such as electric vehicles, cordless power tools, and mobile computing devices. The motivation for MIT Motorsports selecting cylindrical 18650 size lithium ion cells over lithium polymer cells comes down to manufacturing consistency, safety, reliability, and integration with existing technology.

All batteries, regardless of chemistry or type, produce heat when current flows through them in either direction, during charging or discharging. The source of this heat is inherent to the battery cell's construction of physical materials that have electrical resistance. Though in the range of tens of milliohms for typical 18650 cells, joule heating of several watts per cell is possible to sustain long enough with moderate current draw to elevate battery temperatures to dangerous levels. For 18650 cells in common use, these levels are typically measured at the surface of the can and if exceeded will degrade the internal chemistry of the battery and significantly increase the chance of thermal runaway and fire. With hundreds of cells enclosed in each pack, there is very little surface area to reject heat to the environment through convection. Thus, active cooling is required for any high performance electric FSAE vehicle.

2.1   Functional Requirements

For competition use by MIT Motorsports, the battery architecture must meet a number of thermal, electrical, fluid, structural, and manufacturing requirements dictated by the competition rules, the performance demands of the vehicle, and capabilities of the team members to construct in-house. Note that the relevant sentiments of these requirements are captured here, but the precise requirement values used to formulate a finished design are outside the scope of this thesis, where the intent is to explore initial validation of a new design concept.

2.1.1   Practical

The typical timeline for an FSAE vehicle encompasses 9 months of design and manufacturing followed by several months of testing before entering competition. Components may be sourced from external suppliers but the majority of mechanical parts are manufactured and assembled in-house with student accessible resources. The battery design must abide by the limitations of the typical resources of the student team and designed for manufacturing in low quantity. In alignment with performance racing components, there is a necessary requirement for the battery pack to be as small and light as possible to reduce overall vehicle size and mass, improving power density that translates to higher acceleration capabilities, faster lap times, and lower energy use awarded points by the competition events. FSAE electric vehicles typically require battery packs in the range of 21.6-36 MJ (6-10 kWh) of energy capacity, translating to 600-1000 18650 cells at a typical energy content of 32.4-36 kJ (9-10 Wh) per cell. For this reason, the design must be scalable to include a large number of cells while remaining compact and easily manufactured by students.

2.1.2   Thermal

From a thermal perspective, the battery pack must operate in ambient temperatures from $0 - 35°C$ governed by winter conditions in the Cambridge area and the air temperature recorded track side at the competition in Nebraska and California.

Further, the FSAE rules state that cells are not permitted to exceed $60°C$ measured at the surface, concurrent with the recommendations of many cell datasheets provided by the manufacturers. It is important to note that several cells on the market such as the Sony VTC6 are permitted per datasheet to run at an absolute maximum at $80°C$, with implications of reduced lifetime and increased fire hazard. For a large pack consisting of hundreds of cells dissipating several watts of thermal power each, this requires the cooling system to support a maximum heat rejection to ambient on the order of several kilowatts.

2.1.3   Electrical

The competition rules stipulate a maximum pack voltage of 600 V with a maximum discharge power of 80 kW. Electrical isolation of the tractive system and battery pack is continuously monitored by a Bender Isometer IMD-3204 isolation monitoring device, which triggers a fault condition when isolation from the positive and negative battery terminals to chassis is less than 200 kOhms. Similarly, a battery management system must continuously monitor all cells in the pack for fault conditions including exceeding voltage upper and lower bounds, exceeding temperature limits, and loss of any cells in the pack.

2.1.4   Fluid

The only permitted fluids for cooling of the tractive system (encompassing motors, motor controllers, and battery packs) are oil and pure water, with no additives permitted. Materials in contact with the cooling fluid must therefore be chemically compatible and selected to avoid galvanic corrosion to ensure adequate lifetime of the design throughout the racing season. Further, discharge of any kind of fluid throughout dynamic events is not permitted and the vehicle must be operable in rainy conditions without any isolation loss, requiring adequate seal durability against ingress of external fluids and any internal leaking from the cooling system.
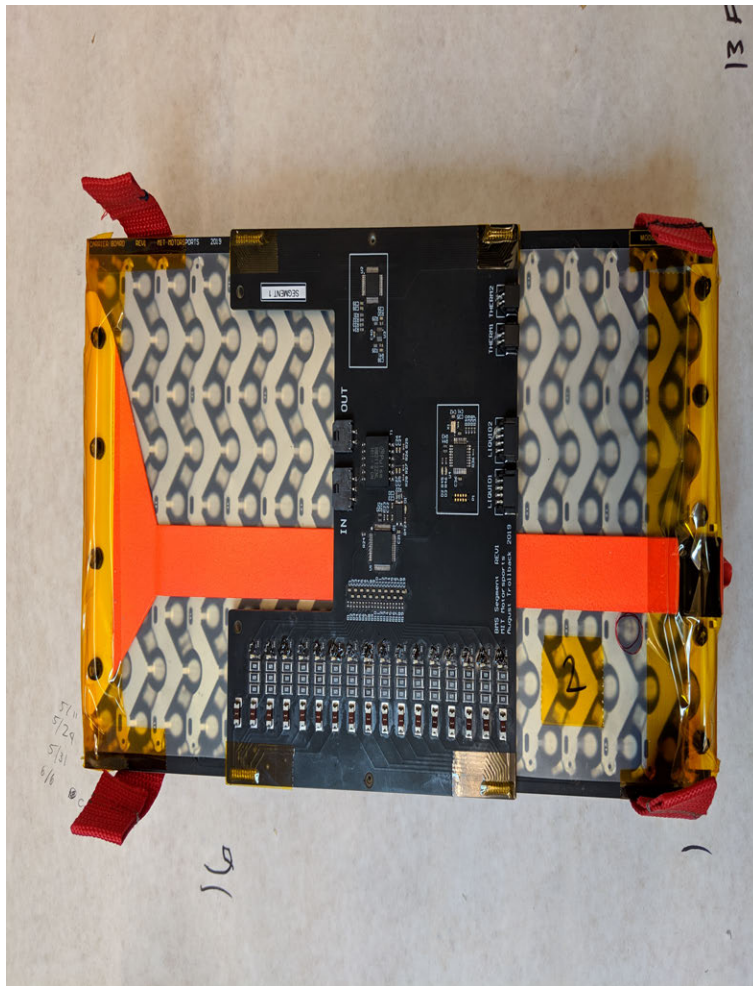
Figure 2-1: An My19 battery module, with custom-designed battery monitoring system (BMS) visible on top.

2.1.5 Structural

During normal driving, the vehicle and battery pack is subjected primarily to vibration loads and inertial loads. Tight integration with the vehicle chassis may also impose twisting and bending loads into the battery structure, which must be routed away from critical interfaces to avoid failure of fluid seals and cell connections. There is also a very real risk of a crash scenario with another vehicle or object. The rules stipulate the battery pack structure must withstand a 40G lateral and 20G vertical load without the pack enclosure separating from the vehicle or rupturing.

2.2 Heat Generation in an FSAE Battery Pack

Using the MY19 vehicle as an example we can evaluate the heat generation during an endurance race. The MY19 battery pack is comprised of 864 Samsung 30Q battery cells with an empirically evaluated DC internal resistance of 23 milliohms and approximate energy content of 36 kJ (10 Wh). The cells fully charged are 4.20 V and 2.50 V when fully discharged. The MY19 vehicle is designed to operate at an RMS power of 20-30 kW, with peak power of 80 kW drawn from the battery pack. At the cell level, this computes to 23.15 W to 34.73 W RMS drawn from each cell over the course of 15-20 minutes.

Using the lower bound power of 23.15W, Ohm's law shows that at when fully charged to 4.20 V the resulting current draw is 5.51 A resulting in 0.70 W of heat generation. At the end of the race when the cell is nearly depleted, 2.50 V corresponds to 1.97 W of heat generation. Using the upper bound power of 34.73 W, this corresponds to 1.48 W and 4.19 W of heat dissipation respectively. For a full vehicle pack, this bounds the heat generation from approximately 600 to 3600 W for a reasonable vehicle.

Refining the cell model with a discharge simulation that takes the energy dependence of the cell voltage into account and the heat capacity of the cell, we can see how the cell temperature evolves over time in adiabatic conditions. Here the cell is modeled with an ideal battery cell in series with a resistor representing the internal

resistance. The voltage of the ideal internal cell is defined as Voc and the voltage measured at the terminal of the cell as Vcc. The cell is connected in series with a constant power load, representing the drive system of the vehicle. Using Ohm's law we can derive relations between the power drawn from the cell, the current in the circuit, Voc, Vcc, the heat generated by the internal resistance, Qdot. Coupling a thermal model of the cell as a heat reservoir with specific heat capacity C = 830 J/kg-K and measured mass M = 0.045 kg, the temperature rise of the cell over time can also be evaluated. [3]
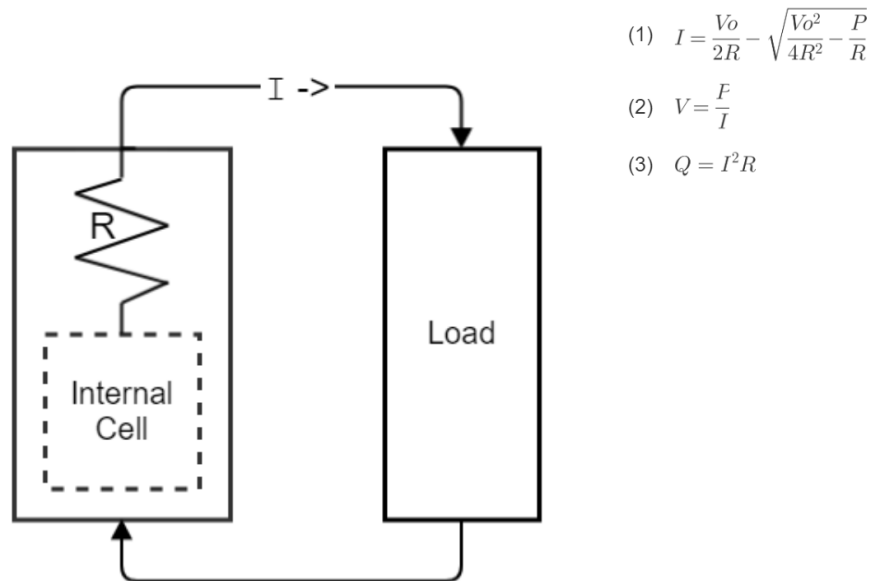
$$(1) \quad I = \frac{Vo}{2R} - \sqrt{\frac{Vo^2}{4R^2} - \frac{P}{R}}$$

$$(2) \quad V = \frac{F}{I}$$

$$(3) \quad Q = I^2 R$$

Figure 2-2: Simple electrical model of a battery cell accounting for internal DCIR.

Running the simulation with a constant 34.73 W load, a cell internal resistance of 0.024 ohms (empirically measured Samsung 30Q), and 1 second discrete time steps until the cell voltage reaches cutoff at Vcc = 2.5V, we can see the adiabatic cell has risen in temperature by 64.6 degrees. Given the cell temperature limit of $60°C$, the cell would have to start at -4.6 degrees to avoid exceeding the temperature limit! While allowed, chilling the cells to below ambient temperatures before the start of the endurance race is very impractical given competition logistics where the environmental temperature at the beginning of a race can exceed $30°C$. Imposing an initial

temperature of $30°C$, we can see the cell will overheat at 485 seconds, at which point only 46 percent of the available 36 kJ (10 Wh) of energy has been utilized. One solution is to add additional cells to the pack to reduce the power per cell and increase overall heat capacity, but this is a very inefficient solution that comes at huge cost to size and mass.
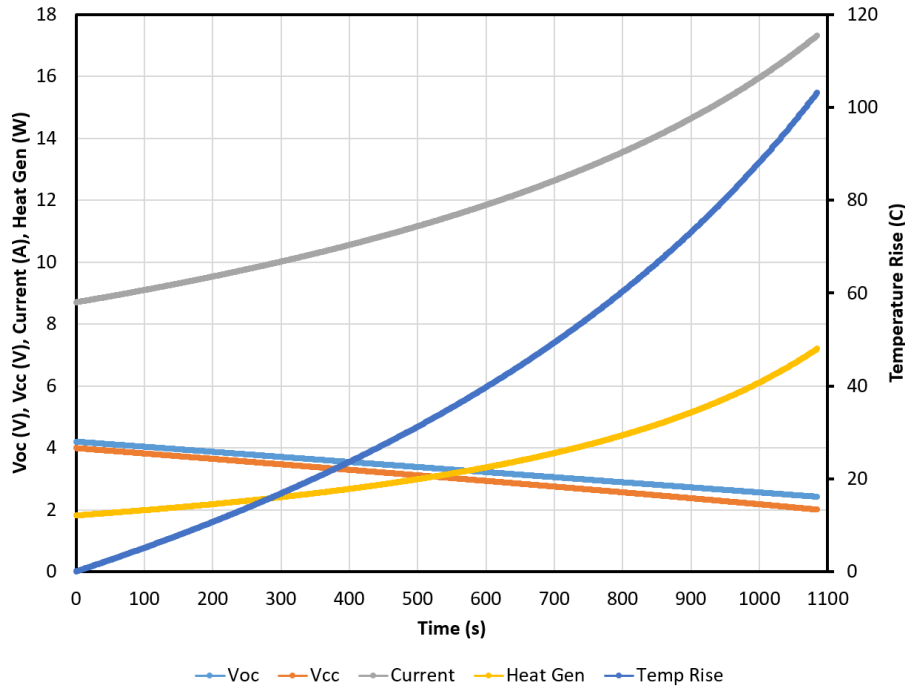
Figure 2-3: Adiabatic discharge simulation of Samsung 30 Q cell at 34.73 W CP load

The coarse model above has many limitations to accuracy. Primarily, the model does not capture the real voltage-energy discharge curve that is relatively poorly approximated by the linear model used. Additionally, the internal resistance of the battery cell varies with energy content and temperature, coupling into the voltage and heat generation calculations. The model also does not take into account heat generated by the resistance of the bus bars or spot weld connections or heat sunk into surrounding structure of the battery module. Despite these limitations, the simulation does provide a starting point for evaluating the performance requirements of a battery cooling system and does capture the bulk source of heat generation in the system. The adiabatic assumption is relatively accurate to actual operating conditions, as each cell in the pack is surrounded by other cells and has very poor thermal contact

with ambient air, impeded by the complete enclosure of the battery cells that does not allow for natural convection.
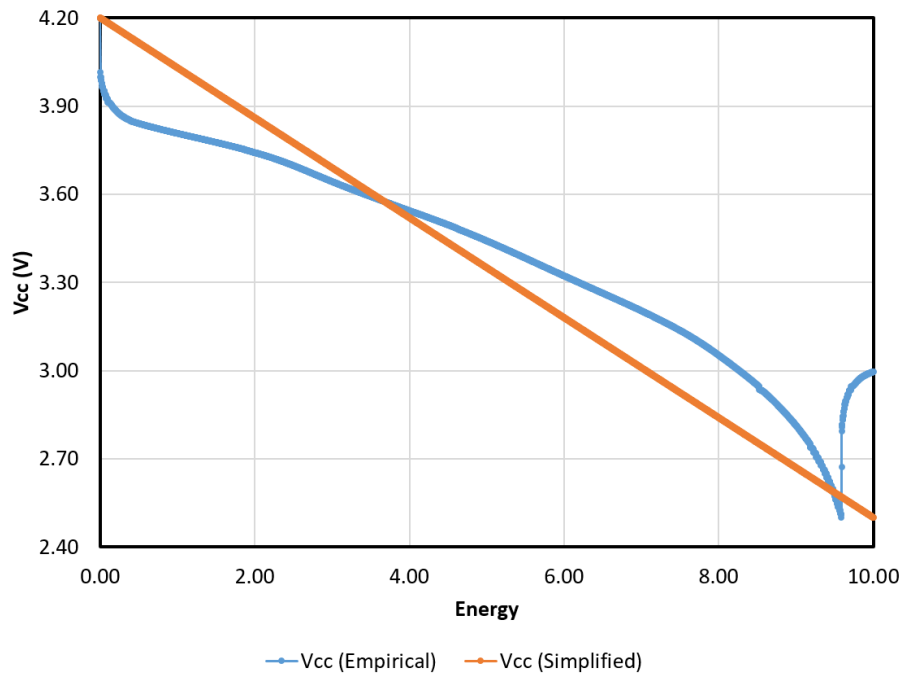
Figure 2-4: Simplified vs empirical voltage vs energy curve of Samsung 30Q cell under 34.73 W CP load.

2.3 Axial vs. Radial Cooling

2.3.1 18650 Internal Structure

With a desire to extract heat from the battery, there are three available surfaces to conduct heat away from the cells: the top, bottom, and side of the cylindrical can. Looking inside an 18650 cell reveals the internal structure, via CT scan. The casing is a drawn steel tube with nickel plating, filled with alternating layers of electrodes, electrolyte, and insulator wrapped in a tight spiral known colloquially as the "jelly roll". The jelly roll contains the stored chemical energy of the cell and the electrode foils are bent and welded to the terminals of the cell at the top and the bottom as positive and negative connections. Heat is generated throughout the jelly roll as a product of chemical reaction and electrical resistance of the electrodes themselves as

current flows to the terminals.
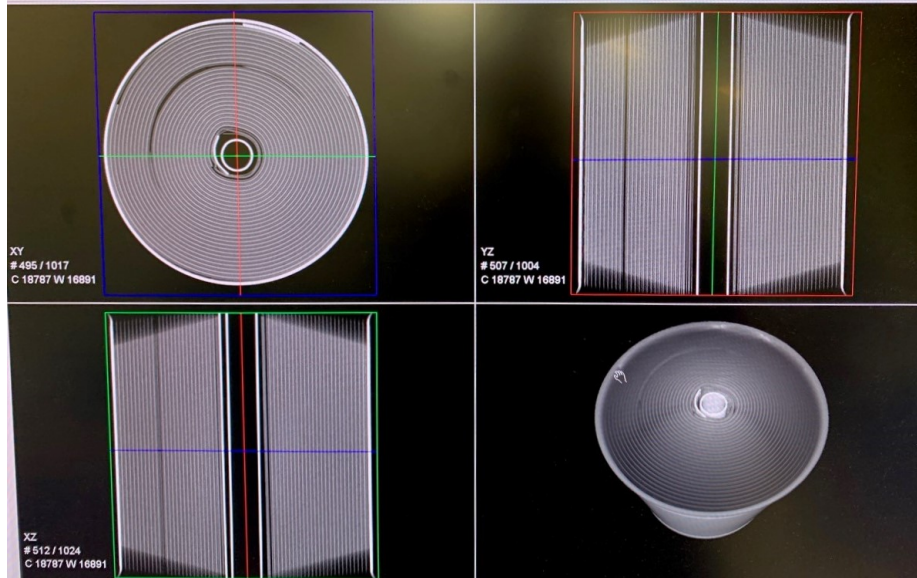
Figure 2-5: 3D CT scan of Sony VTC6 cell revealing the jelly roll construction within the steel can.

Looking in the radial direction from the center, there are alternating layers of insulator and electrode material until the steel can is reached. Heat generated in the jelly roll near the center must conduct through the many layers to reach the outside. Looking axially, heat generated in the layers of the jelly roll can conduct through the solid metal material of the electrode before reaching the ends of the cell. At the anode end (bottom), the bottom tabs are welded to the base of the can after folding around a thin cloth disk that prevents the layers of the jelly roll from shorting out. This also functions as a thermal insulator. At the top of the cell is a carefully engineered pressure vent, current interruption device, gasket, and formed sheet metal that closes off the open end of the steel tube. Thermally, there are a lot of elements for heat to transfer through to reach the top side of the cell and this is the only place to electrically connect to the positive terminal, making it undesirable for conducting heat away from the cell.

Figure 2-6: Teardown of the 18650 cell reveals the jellyroll construction and insulators on each end.

2.3.2 Modeling Conduction

The conduction resistance in each direction can be modeled as a resistive network with series resistors for each material change and contact resistance. In the axial direction, there are few layers overall but much smaller area for conduction with a large resistive gap at the bottom between the jelly roll and the bottom of the can. Radially, there are many very thin layers with contact resistance between but a much larger surface area. Analytically evaluating radial and axial conduction is possible but the properties of the materials inside are not easily available without significant materials testing. Instead, it is more accurate to test the radial and axial conductivity of the cell as an assembly through empirical means. Previous research provides experimental values of radial conductivity Kr = 0.2 W/m-K and Kz = 32 W/m-K. [3]

Using these figures, it's evident the cell is much more conductive axially than radially. The bottom of the cell has an exposed area of $0.000266m^2$, compared to the side where $0.0003757m^2$. This exposed area is 14x higher and attractive for

28

Figure 2-7: Teardown of the bottom side of the 18650 showing the anode end insulator.

heat transfer, but the significantly higher conductivity in the axial direction is also desirable. One figure of merit is to multiply the exposed area by the directional conductivity and divide by the mean length from the heat source to the surface to produce an effective conductivity-area per unit length metric in units of W/K. Computing these numbers shows a slightly higher value for radial cooling, but at the expense of requiring the entire surface area of the cell to be utilized. Axial cooling is nearly as effective with much less area on only one side of the cell and is practically very attractive in terms of manufacturing complexity.

Parameter	External Area mm^2	Conduction Distance mm	k (in direction) W/m-K	kA W-m/K	kA/L W/K
Radial	3757	9.2	0.2	0.00075	0.083
Axial	266	32	32	0.00532	0.166

Figure 2-8: Axial vs radial conduction figures of merit.

One drawback of end cooling is the significant gradient in temperature that will be produced in the cell since heat is being drawn only from the bottom. Necessarily, heat at the top of the cell will not reach the cold plate as effectively and the cell will

increase in temperature at the top. This internal temperature gradient has potential consequences for energy content and cycle life of the cell, and is a topic for further research.

2.3.3   Practical Implications

From a design and manufacturing perspective, cooling even a portion of the cell's radial surface is much more difficult compared to the bottom side. The curved surface requires complex geometry for heat exchange with a fluid, and increasing the radial spacing of the cells to allow space for fluid flow rapidly increases the size of the battery module, pack, and consequently adds mass. In contrast, the bottom end of the cell is planar and allows for minimum cell spacing to minimize pack volume and maximize energy density of the system.

3

Proposed Design

FSAE battery packs are built of smaller modules that are connected together electrically and mechanically in an enclosure to form a higher voltage pack. Separation into modules reduces the maximum voltage, energy stored, and physical size of each discrete unit, easing prototyping, design, and manufacturing overall while improving safety and usability by allowing for isolating problems and swapping out components without addressing the entire potential of the entire battery array at once. Battery design evolves at the module level, allowing for refinement and testing at a smaller scale before investing in assembly of many modules to form a large pack. Though this design is for a 144-cell module, development testing was conducted with quarter-scale module components consisting of 36 cells in 6S6P configuration to allow more rapid iteration and testing.

3.1   Concept

This novel module design consists of an array of 144 18650 battery cells arranged with 16 banks of cells connected in series, each bank consisting of 9 cells connected in parallel. All cells are oriented vertically in the same direction, with cell connections and monitoring hardware all residing at the top. At the bottom of the cells is a cold plate assembly comprised of a base plate with a U-shaped flow geometry and a top plate to form an enclosed cavity. The cold plate is assembled with male dovetails in

the base plate joined to female dovetails in the top plate, bonded and sealed with silicone RTV adhesive to form a water-tight flow cavity. Fluid fittings are attached with G-1/4 threads in the top sheet, allowing use of off the shelf fittings designed for water cooling personal computers, such as those sold by Koolance that utilize a recessed o-ring for sealing. The base plate is CNC milled from aluminum and the top plate is a sheet of metal-core printed circuit board (MCPCB) material that has been CNC milled to mate with the base plate.

The MCPCB material, provided by Polytronics as TCB-C, is a three-layer composite, consisting of an aluminum substrate, a polymer ceramic insulator, and a copper foil. The ceramic layer electrically isolates the copper foil from the aluminum substrate, critical for the typical use of MCPCB material as a printed circuit board without forming short circuits. MCPCB materials are designed for use in high power electronic devices such as power converters, motor drivers, and LEDs that generate large amounts of heat and must be sufficiently cooled to operate. Normal fiberglass PCBs in this case are much more insulating and do effectively conduct heat through the circuit board away from components. Substituting for an MCPCB allows much greater thermal dissipation by replacing the fiberglass composite with a sheet of aluminum, but requires the ceramic interface layer to isolate the circuits etched into the copper foil from shorting out.

The copper foil of the MCPCB is etched with a triangular grid pattern of circles that matches the cell array, then electroless tin plated. The cells are electroplated with copper and tin and soldered to the MCPCB grid with bismuth-tin solder alloy. The solder joint forms a purely mechanical connection and is the conductive path for heat to transfer to the fluid cavity.

The cells are connected at the top with chemically etched nickel foil current collectors resistance spot welded (RSW) to the center (cathode) and rim (anode) terminals to form series-parallel connections. The current collectors integrate fuse geometry that protects each individual cell from overcurrent conditions. The current collectors are isolated from shorting the cells inadvertently by a carrier PCB that is bonded to the top of the cells with a sheet adhesive. The carrier PCB masks the cells in all areas

except where the current collectors need to bend down and make spot weld connections. The PCB also has an array of 30 thermistors that protrude in the interstitial volume and are potted between cells to accurately measure cell temperature. Thermistor connections and cell voltage sense connections are broken out to four headers on the PCB for connection to external test equipment and battery management hardware.

3.2 Cold Plate Architecture

Packaging cells into modules in a rectangular array exposes the ends for attachment to a cold plate. The cold plate needs to be as thin and lightweight as possible to reduce module size and maintain vehicle density, while simultaneously acting as the structural interface between the cells and the pack structure. The cold plate should also enclose the minimum possible volume of coolant to reduce fluid mass. This pushes design towards a very thin, sturdy cold plate with a very good thermal interface to maximize heat transfer efficiency. It is also important to minimize the pressure drop across the cold plate to maximize fluid flow velocity, which directly improves convective heat transfer. The simplest and highest performance solution is to have the coolant directly in contact with the MCPCB to minimize mass and save space and material. This is also desirable to decrease the amount of metal used and maximize the volume used by water in order to decrease the flow resistance and minimize overall mass.

The simplest design would be to form a thin rectangular coolant channel by attaching a five sided box at the edges to the MCPCB, forming a sheet passageway at the bottom for coolant to flow in one direction. The edges could be sealed by a gasket, elastomer, or adhesive and fittings attached at the ends. In this simplistic design, even a small amount of pressure acting on the large surface area of the enclosed volume would rapidly build up hundreds to thousands of Newtons of force trying to inflate the cold plate and burst the seams. Regardless of joint failure, the pressure load acting on the thin MCPCB will cause it to deform and bow upwards,

possibly compromising electrical connections and causing leaks. The low stiffness of the system can also activate a harmonic drum mode coupled with vehicle vibration and introduce even higher vibration forces in the structure.

Adding support ribs in the center improves structural properties at a minor cost of mass, but bonding to the MCPCB in the center of the fluid passage is difficult with traditional means – fasteners require penetration of the MCPCB and access from the other side, presenting dangers of electrical shorts and fluid leaks into the cell cavity with almost no space available between cells for hardware. Adhesives similarly require a large bond area to develop enough tensile stiffness for the joint to remain strong and have minimal deflection under pressure load. Sealing the edges with a gasket and hardware similarly requires space allocated for the seal surfaces, features, and clamping hardware.

Another consideration in the simple design is the unidirectional flow path. This will necessarily cause the coolant to heat as it travels from the beginning of the module to the end, causing a corresponding rise in temperature of the cells in the same direction. A multi-pass cold plate in a U or S shaped configuration helps mitigate temperature differences by allowing fluid to transfer heat to adjacent channels, but at the cost of an increased flow resistance by adding surface area and bend losses.

The proposed design attempts to mitigate the challenges and tradeoffs of optimizing material efficiency, thermal performance, size, weight, and sealing complexity by use of sliding dovetail interfaces and silicone adhesives. The flow cavity is a U-shape to provide even temperature across the module without too much flow restriction, utilizing the center partition and several flow straighteners as mechanical supports to attach the bottom plate to the MCPCB. The outer edges of the cold plate, the center partition, and the flow straighteners are machined with very small male dovetails that mate to female dovetails machined partway into the MCPCB. The two structures can slide together to form a closed flow cavity, sealed by filling the gaps in the dovetails and slots in the ends with silicone RTV adhesive. When cured, the pressure load of the coolant attempts to split the MCPCB from the bottom plate, but the dovetails utilize the strength of the aluminum to take the load by putting the silicone adhesive

34

in compression where it is much stronger and stiffer. Restricted by the geometry of the dovetails, the cold plate actually seals tighter when more pressure is applied until the silicone material eventually fails. The silicone is also highly elastic, allowing for twisting and minor movement between the MCPCB and the base plate induced by mounting to the pack structure and any vehicle loads that deform the cold plate. This intended compliance prevents the cell joints with the MCPCB from cracking under loads passed through a stiff bolted connection to the cold plate.

3.2.1   Fitting Choice

Lastly, the fittings are selected to provide robust sealing and serviceability. Threading ports in the MCPCB allows all interfaces with the module to be top side accessible for easy maintenance and manufacturing. The very thin material of the MCPCB and cold plate base would not be able to seal effectively with NPT type tapered threaded fittings due to the very high install forces and spiral leak path. Instead, straight thread elastomer seal fittings are used to provide positive sealing with good durability to be replaced without concern for material failure under the high stresses of a tapered thread. G1/4 fittings used for PC water cooling in particular utilize a soft o-ring that is very compliant and seals tightly to smooth surfaces with minimal torque requirements, and are available in a wide range of very compact fitting types. The G1/4 thread pitch is also 1.3 mm, allowing for just over a full thread of engagement in MCPCB material.

3.3   Cell to Cold Plate Interface

The critical interface in a liquid cooled battery design is maximizing heat transfer from the battery cells without compromising electrical isolation. This is compounded by the common property that most good thermal conductors such as metals are also good electrical conductors. There is a narrow class of ceramic and polymer materials that have high thermal conductivity and good insulating properties such as boron nitride, silicon carbide, beryllium oxide, aluminum nitride, etc. that are

often used in refractory environments, as high performance coatings, and are in some cases used as thermal interface materials. All of these materials are relatively difficult to obtain in bulk solids and their brittle nature is not conducive to manufacturing into custom forms for engineering use without very high costs. Further, the problem still remains to provide good thermal contact and mechanical coupling between the interface material and the cell. One approach is to use an extremely thin layer of a good electrical isolator with poor thermal performance, such as plastic heat shrink film or epoxy adhesive. Minimizing the layer thickness maximizes net thermal conductivity to the coolant at a cost of manufacturing complexity – these layers are often needed on the order of 100 microns or less with no tolerance for gaps or thickness variation that can compromise electrical isolation at high pack voltages up to 600V. MY19 was designed with a 100 micron layer of epoxy adhesive as the only separation between the cells and the aluminum cold plate, and ultimately suffered isolation issues due to poor joint reliability. A second version of the pack used Kapton film as an added layer of isolation but still required the epoxy to attach the film-coated cells to the aluminum cold plate, resulting in significantly worse thermal performance overall.

The proposed design utilizes a material that has been engineered to solve this exact thermal interface problem. As mentioned previously, the MCPCB represents a mass manufactured composite of an aluminum or copper substrate coated with a very thin, high thermal conductivity electrically insulating polymer sandwiched by a layer of copper foil. The need for these materials to support development of high power electronic devices drove investment into the manufacturing process to create the high performance polymers and laminate them onto traditional metal panels into a package that is extremely consistent, high performance, dimensionally flat, and very inexpensive. The design intent to be compatible with PCB manufacturing processes also offers exciting prospects for scaling up this design concept utilizing existing infrastructure and integrating embedded circuitry directly into the cell array with high fidelity. A comparison of available interface approaches is compiled in the table below (Exotic ceramic materal properties, adhesives/epoxies properties, MCPCB properties, costs for all, include an MCPCB cutaway).

36

3.3.1 Adhesives

Even utilizing an MCPCB as an interface material to provide high thermal conductivity and electrical isolation, the problem still remains to effectively attach the cell to the material. The key advantage is that the MCPCB offers metallic surfaces on both sides with a laminated insulator, removing the need for the cell attachment to be electrically insulating. The aluminum is conducive to attachment or construction into a cold plate in a fluid manifold, while the copper foil can easily be etched, plated, and soldered to attach to the cell with a solid metal joint with extremely high thermal conductivity with the isolation layer baked into the MCPCB construction and optimized for heat transfer. Using an adhesive to bond cells to the MCPCB would even in the best case cause huge thermal resistance as even the best thermal epoxies claim only a 1-2 W/m-K conductivity rating, with a minimum recommended bond line on the order of 100-200 microns. Compared to the 12 W/m-K conductivity and 100 micron thickness of the Polytronics TCB-C MCPCB polymer, this is at least an order of magnitude more thermally resistive and would dominate in obstructing heat transfer. [2]

3.3.2 Soldering

Metallic approaches bonding battery cells to the copper foil of the MCPCB are much more attractive. Low temperature solder alloys have good conductivities from 20-90 W/m-K depending on the content and quickly form very strong joints with minimal bond line thicknesses. They are also widely available in many alloys at relatively low cost with a huge range of fluxes, process parameters, and specialty formulations to choose from to achieve optimal results. The downside of soldering is that almost all processes require exceeding the melt temperature of the alloy for several minutes if possible to form quality joints, and with the process temperatures of even low temp alloys in the neighborhood of 120-180   this greatly exceeds the allowable $80°C$ of 18650 cells.

3.3.3   Cold Welding

One briefly explored cold process is indium cold welding. Indium is unique in its ability to cold weld at room temperature and pressure as long as uniform pressure is applied to force indium-plated objects together. Indium can readily electroplate almost any metal including copper and nickel. Unfortunately, development tests detailed later found the plating and cold welding process unsuccessful for this application.

3.3.4   NanoFoil

Another product by Indium Corporation is NanoFoil, marketed as a "rapid, room temperature soldering process". NanoFoil is a reactive multi-layer foil of thousands of alternating layers of vapor-deposited aluminum and nickel. When thermally activated by electric current or laser, the layers react in milliseconds, heating up to $1500°C$ locally and travelling 8 meters per second across the foil. The extremely high temperature is extremely short in duration, allowing soldering and substrate bonding processes to reach suitable temperatures with low enough energy input to avoid the bulk material absorbing any heat. One application for NanoFoil is for bonding sputtering targets that must have low voiding and maintain good flatness. NanoFoil is a perfect candidate for rapidly soldering battery cells to a PCB substrate without any heating of the battery cell. However, NanoFoil is quite expensive and in short supply, making it unavailable for prototype testing.

Figure 3-1: Top view of the MY19 battery pack, showing six battery modules connected in series to form the larger pack.
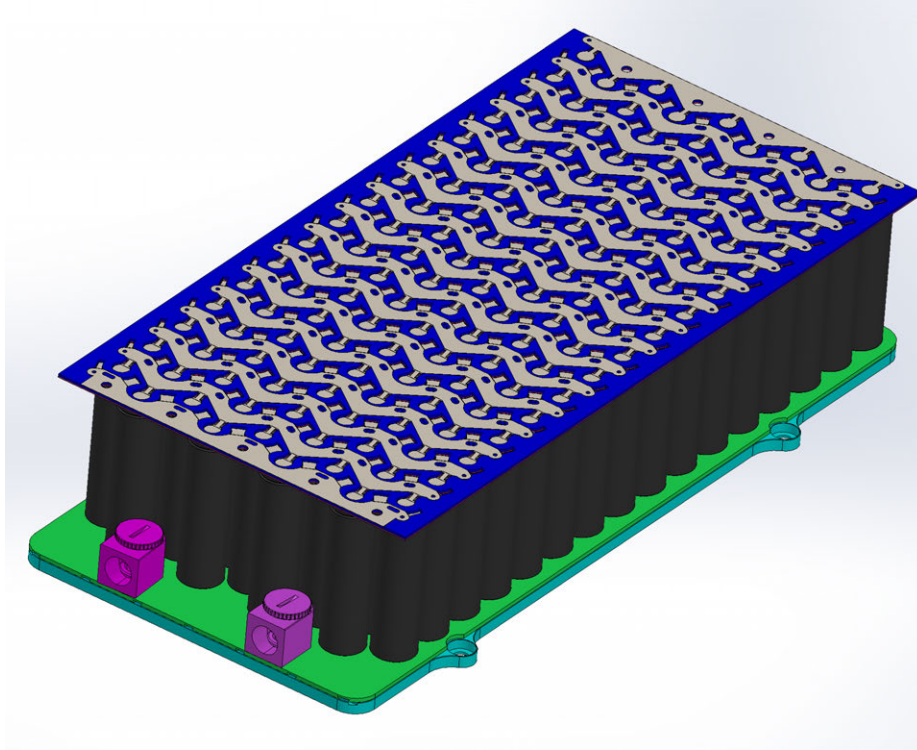
Figure 3-2: CAD model of the novel design. The top blue PCB insulates the nickel foil bus bars spot welded to the top of the cells forming a 16S9P module. The MCPCB (green) and cold plate base (blue) are soldered on to the cell array.
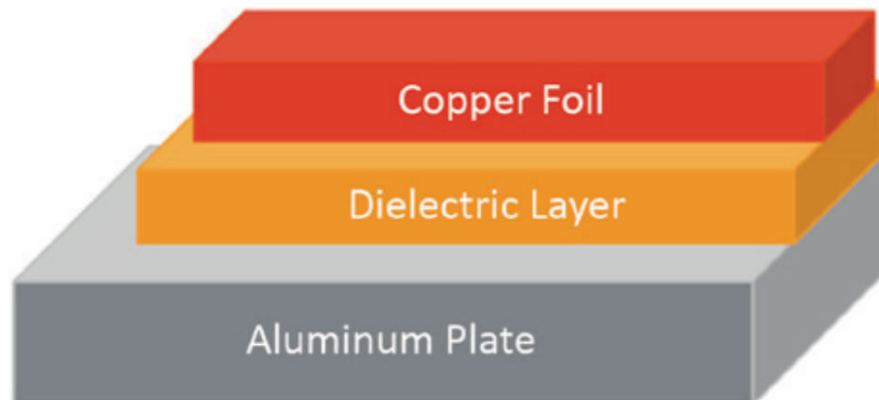

Figure 3-3: Layer breakdown of MCPCB material, also known as insulated metal substrate (IMS).
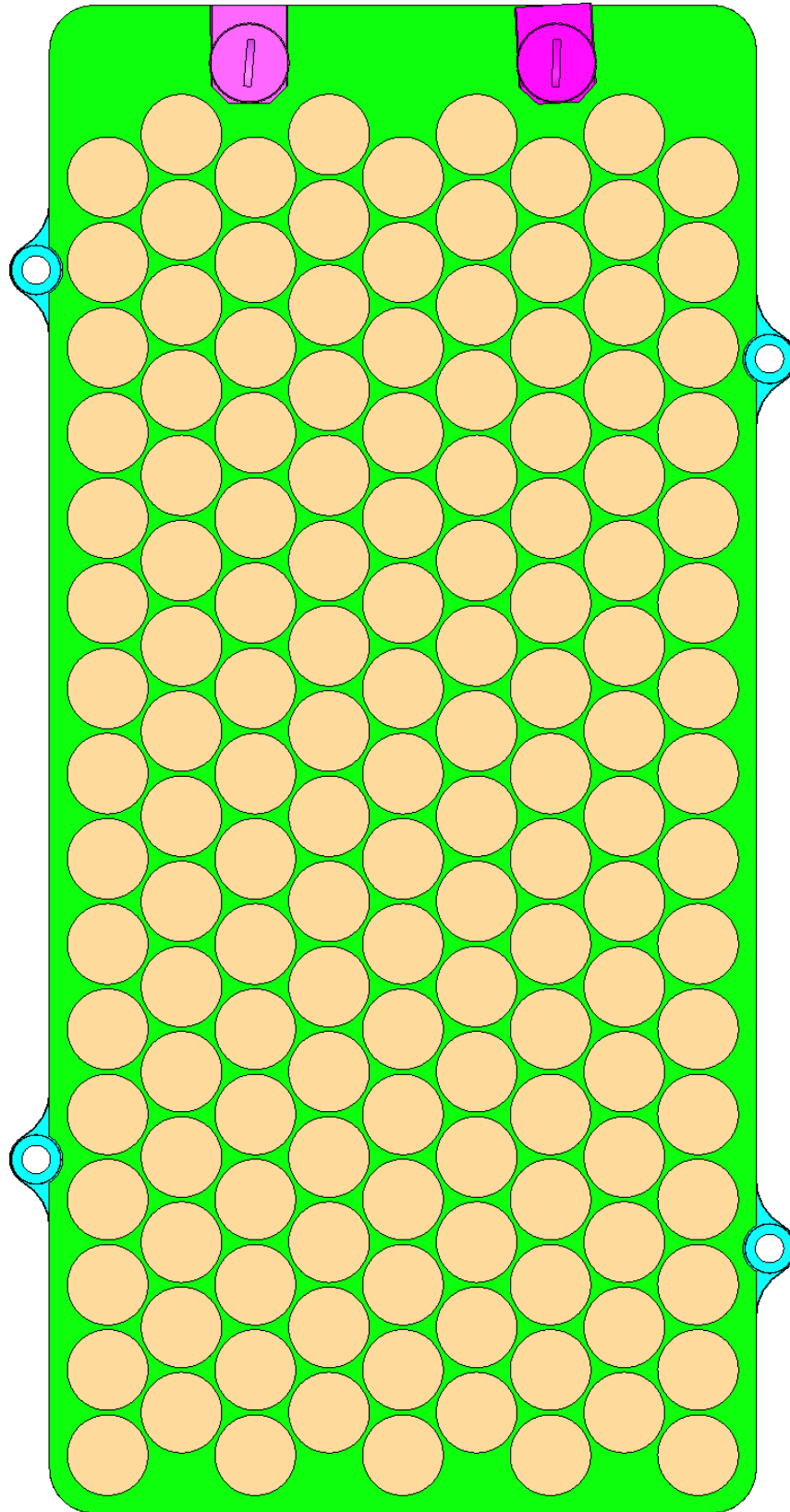
Figure 3-4: Top view of the cold plate assembly, showing the MCPCB etched with copper circles for soldering to individual cells
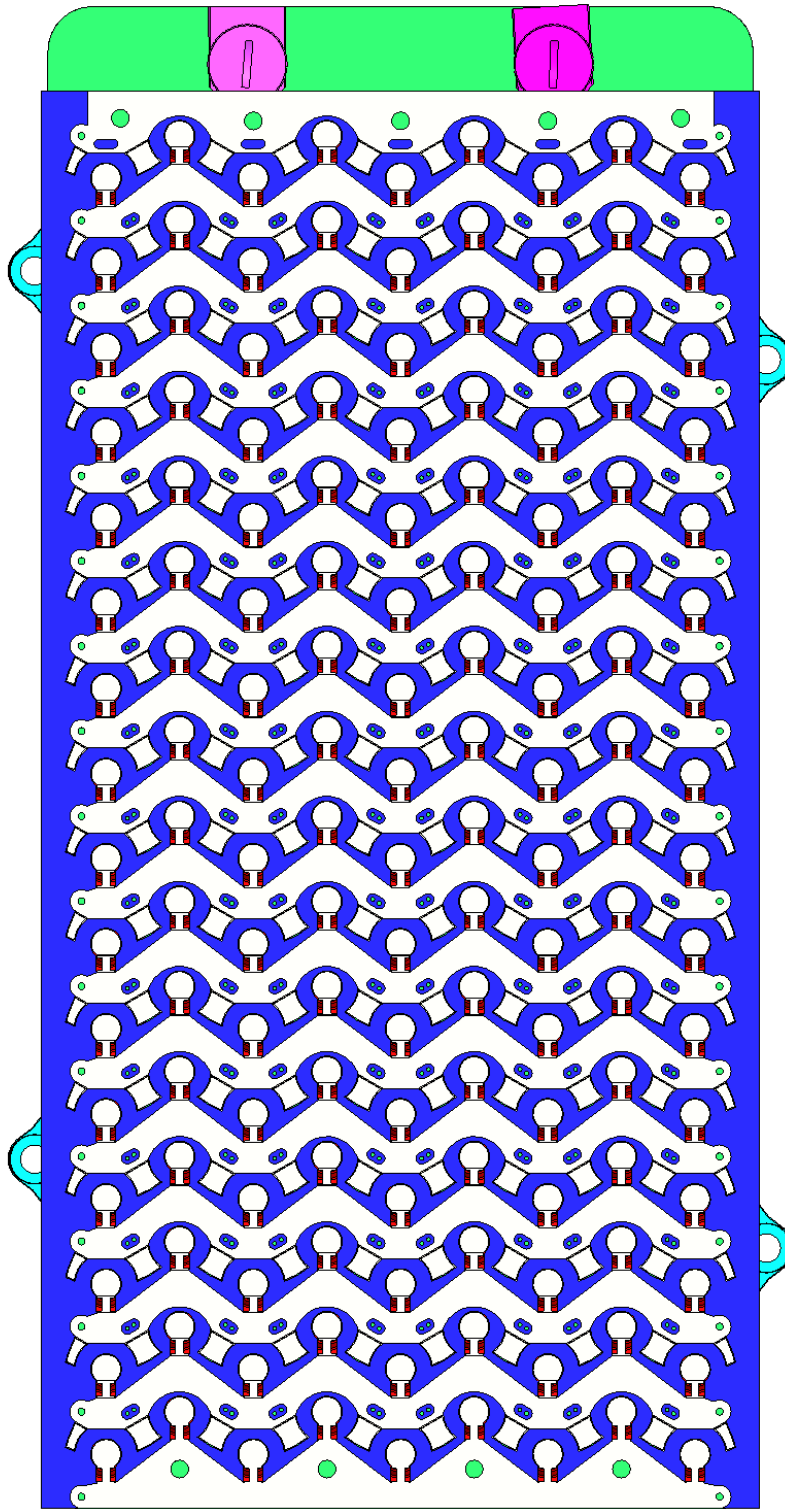
Figure 3-5: Top view of the module design, showing nickel bus bars connecting cells in series and parallel with integrated fuse elements.

Figure 3-6: Section view of the module assembly, showing the cold plate base (blue) dovetailing with the MCPCB (green).
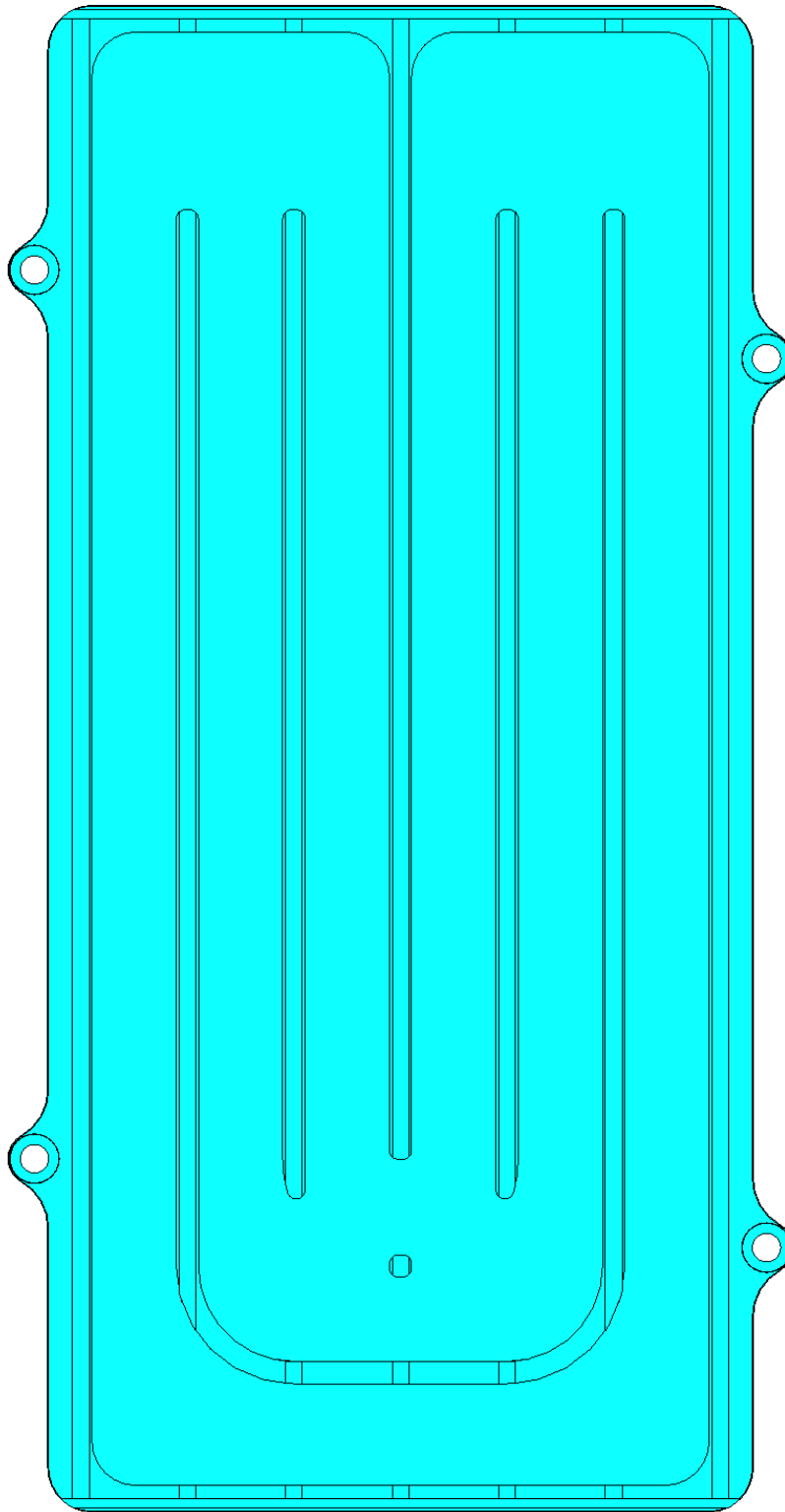
Figure 3-7: Top view of the cold plate base, showing the double U flow channels and center support ribs with dovetails.
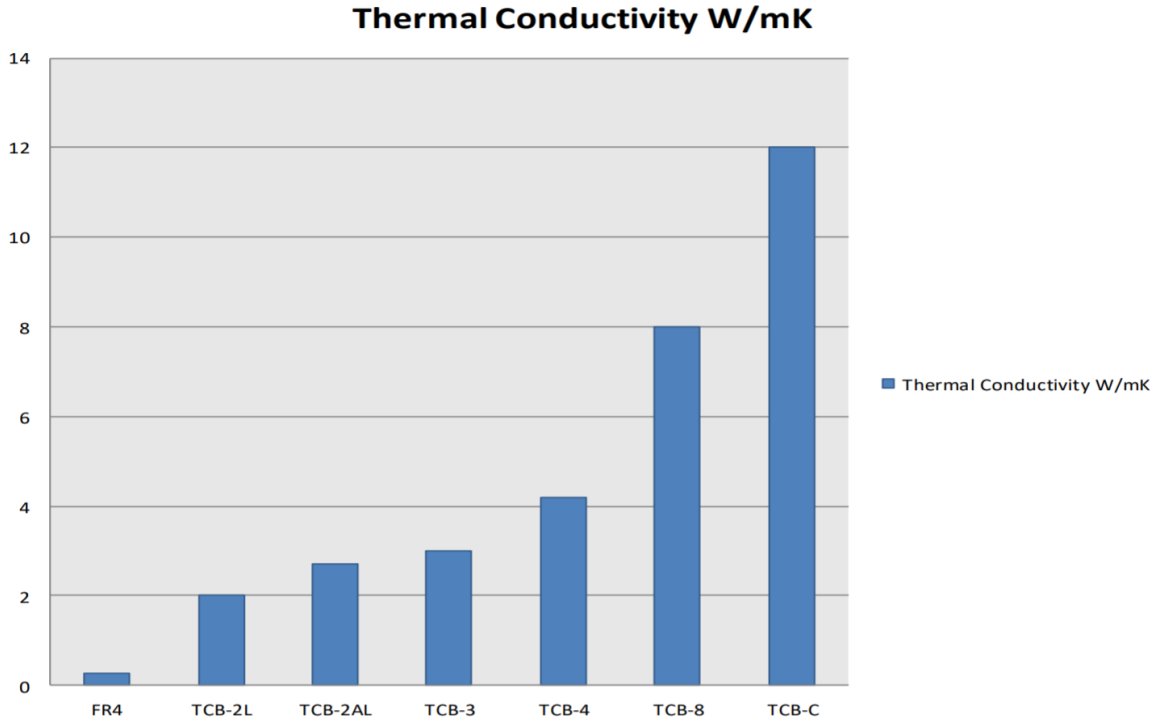
Figure 3-8: MCPCB offerings by Polytronics, with various levels of thermal conductivity available.
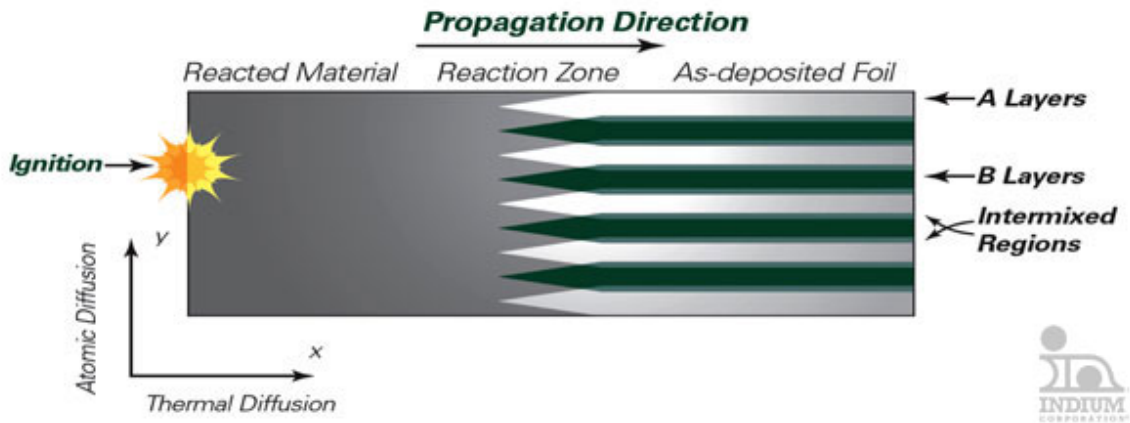
Figure 3-9: Idium Corporation NanoFoil material for bonding substrates.

4

Process Development

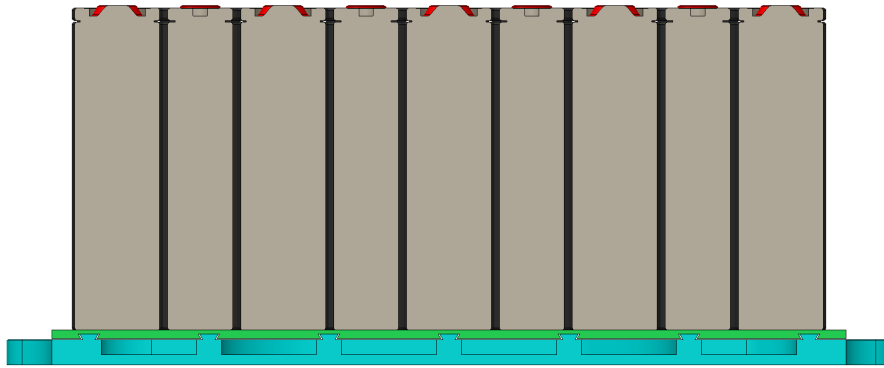A number of test articles and samples were created to investigate the viability of design concepts and converge on manufacturing procedures. These fall into four categories: MCPCB machining, pattern etching, cell bonding, and cold plate fabrication. All testing was conducted on single cell samples or quarter-scale 36 cell modules, with the developed processes intended for use in producing full size 144 cell modules.

Figure 4-1: A 36 cell test module used for development.

4.1 MCPCB Machining

MCPCB material is commercially sold in standard 18 by 24 inch panel sizes for PCB production. The composite material also has very tight thickness and flatness tolerances to ensure process reliability in commercial use. Though the bulk of the material is a solid aluminum substrate, the ceramic layer and copper foil lamination present complications for traditional prototyping methods. Attempts to waterjet the material to rough dimension with an Omax 5555 JetMachining Center were ultimately unsuccessful as the water pressure caused inflating forces that split the copper foil away from the substrate and filled both metals with garnet abrasive.
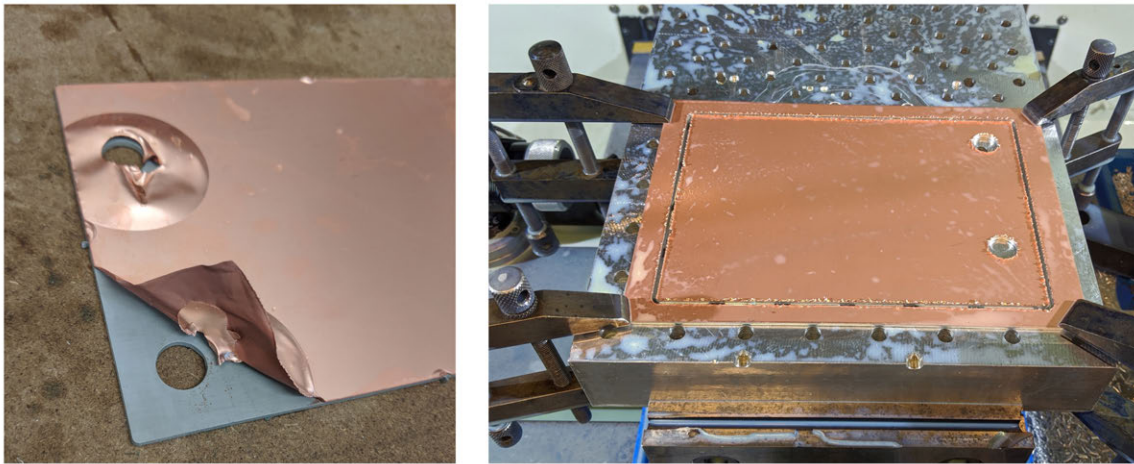
Figure 4-2: Left: results of waterjet cutting attempts. Right: CNC machining.

Instead, it was effective to use a sheet metal shear to rough cut the material and CNC mill all outline and internal features of the part using a Pierson Workholding vacuum plate system in a Haas VF2 CNC machine. 1/16 inch diameter carbide end mills were used to profile the outer dimensions and create internal features, followed by a Harvey Tools 1/8 inch diameter 60 degree dovetail cutter to produce female dovetail channels to mate with the cold plate base. Ports for the fittings were bored with the 1/16 inch end mill and tapped on a manual mil to fit G1/4 threads. The finished features are carefully deburred with a scraping blade and the entire part thoroughly degreased and cleaned to prepare for chemical etching.

4.2   Pattern Etching

4.2.1   Vinyl Cut Mask

The MCPCB material has an interrupted copper foil on one side, intended to be etched into PCB traces with traditional PCB etching fabrication processes. In this design, the copper layer must be etched into circles matching the cell grid, where each cell is independently bonded to individual circles electrically isolated from each other. If the copper was left un-etched, the soldering would electrically connect all the cells in parallel by the bottom terminal, shorting out the module. The pattern could easily be etched by sending the files to a PCB fabrication house, but utilizing exotic or specific materials such as high performance types of MCPCB can add significant costs and lead times to otherwise very inexpensive processes. For this reason, a process was developed to mask and etch the copper pattern in the lab. Because the cell spacing is very wide at 1 mm and there are no fine electrical connections to be made like a traditional circuit board, very coarse methods of masking are viable instead of photolithographic methods used in the PCB industry. In this development process, a Roland CAMM-1 GS-24 vinyl cutter was used to cut masks from adhesive backed vinyl that was transferred to the copper foil surface of the machined MCPCB with transfer film. Chemical resistant tape is used to mask all other exposed aluminum on the MCPCB and a laminator is then used to ensure a strong bond between the mask and copper foil.

4.2.2   Sodium Persulfate Etching

With the triangular grid pattern and aluminum surfaces masked off, the exposed copper can now be etched away by immersion in an etching bath. Sodium persulfate was chosen over other common DIY PCB etchants such as ferric chloride due to low reactivity with aluminum and relatively high etching speed. Sodium persulfate powder was dissolved in deionized water at a concentration of 230 g/L and continuously pumped over the MCPCB in a custom etching tank. The tank is constructed from

Figure 4-3: Vinyl mask cut, applied, and masking the remaining exposed aluminum.

a stainless steel steam pan and DC pump, utilizing chemical resistant fittings and materials to avoid corrosion and leaking. A small heating element and PID controller maintains the etchant at $50°C$ to enable full etching of the copper in approximately 20 minutes. At the end of the etching process, all visible copper has been removed. The MCPCB panels can be thoroughly rinsed in water and all the masking material removed to reveal perfectly shiny copper circles with well-defined crisp edges. The sodium persulfate does not appear to remove any aluminum or polymer ceramic. This process allows for rapid design iteration through use of inexpensive commercially available craft materials to produce a new mask and etch patterns in under 30 minutes, provided the details in the design are no smaller than about 0.5mm in size, limited by the performance of the vinyl cutter used.

4.3   Cell Bonding

The cell bonding development process down selected a wide variety of available fluxes, solder alloys, and electroplating options to a single set of process parameters that produces reliably strong, consistent solder joints from cell to MCPCB. Due to the inability to source NanoFoil, indium cold welding and soldering processes were
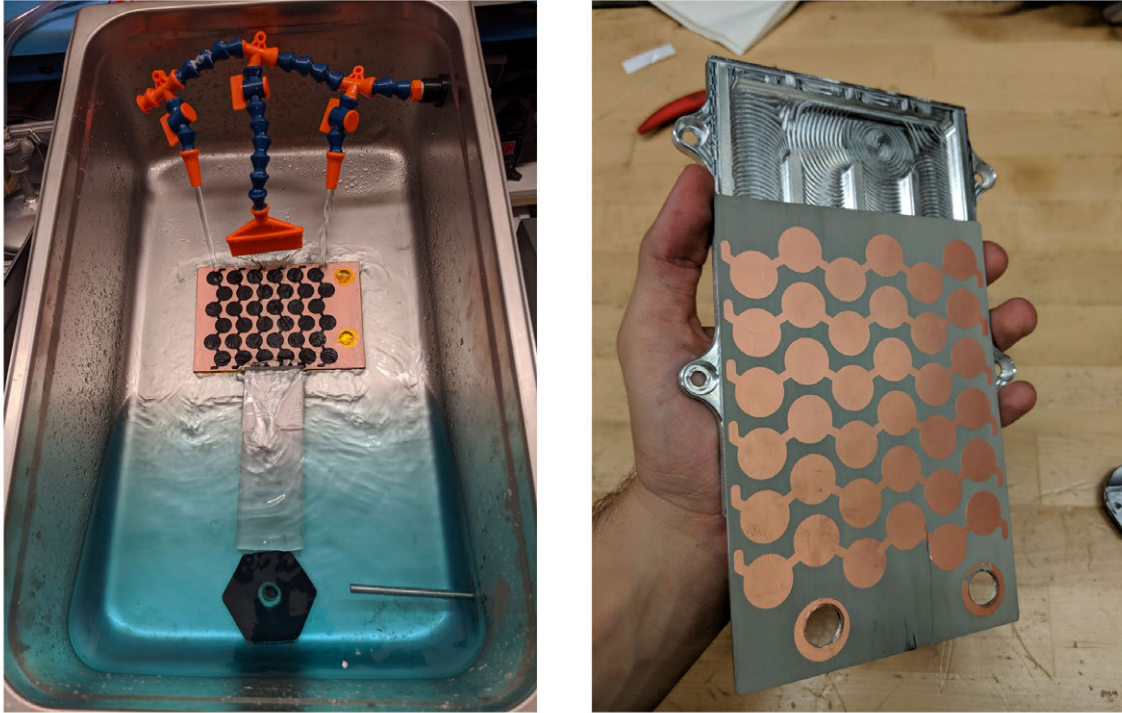
Figure 4-4: Left: sodium persulfate etching tank in operation. Right: End result of etching, leaving copper circle grid behind. Shown assembled onto the cold plate base.

both investigated as viable solutions. A number of indium-based solder alloys were tested by punching sample ribbon into solder preforms in conjunction with commercially available soldering fluxes. After experimentation and decent results, the indium solder alloys were ultimately found to be too costly to scale up beyond small battery modules. Instead, a less expensive bismuth-tin-silver solder paste was found to produce acceptable joints. The indium alloy solder experiments will not be covered here.

4.3.1 Soldering Equipment & Procedure

Chosen for the low cost and reasonable melting point, paste has an optimized flux carrier and can be precisely dispensed by screenprinting, manual syringe dispensing, or by automated CNC dispensers. An important consideration was the ability to scale up to full size modules with automated placement and dispensing using a custom made CNC solder paste dispensing machine capable of producing perfectly repeatable and volumetrically consistent dots of solder paste exactly in the center of each solder pad

of the MCPCB. The dispensing machine is built on a Genmitsu 3018-PRO router kit with GRBL controller, modified with an onboard Raspberry Pi 3B+ running bCNC. The engraving spindle was replaced with a DM Dispenser solder paste dispensing syringe kit available on Tindie, with dot dispensing triggered by the spindle control of the CNC controller. An upgraded table with corner guide and homing switches allow for writing g-code programs to dispense solder paste in any dot size or location within the work volume.
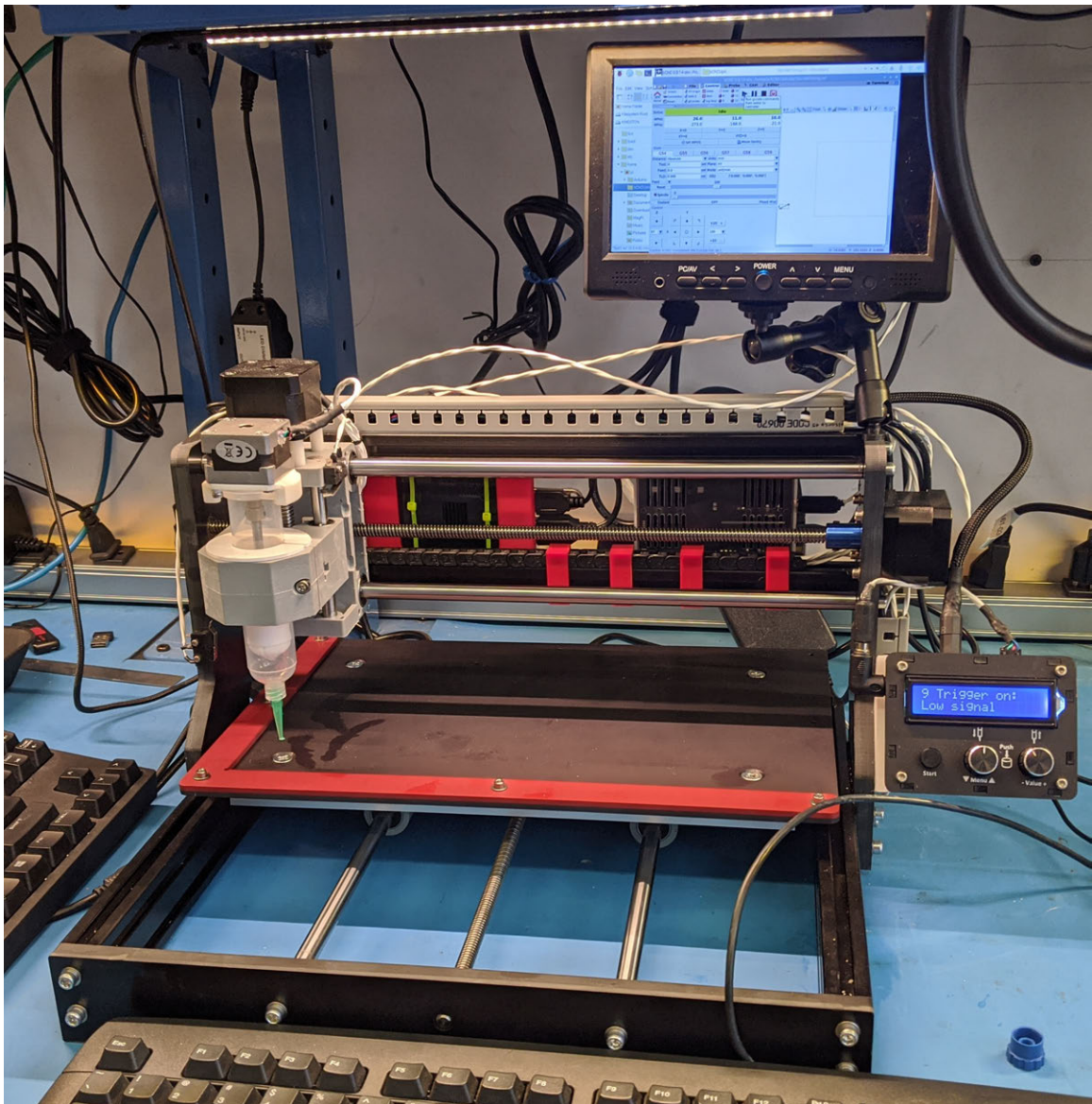

Figure 4-5: DIY CNC solder paste dispenser built on an inexpensive CNC engraver platform.

Samples were soldered using a custom built hot plate that integrates a liquid cooling loop to facilitate extremely rapid cooling after the soldering process is complete. The hot plate is constructed of a 5 by 12 inch Wakefield Vette multi-pass buried tube cold plate with two 350 W strip heaters bolted to the bottom side and insulated with mineral wool.
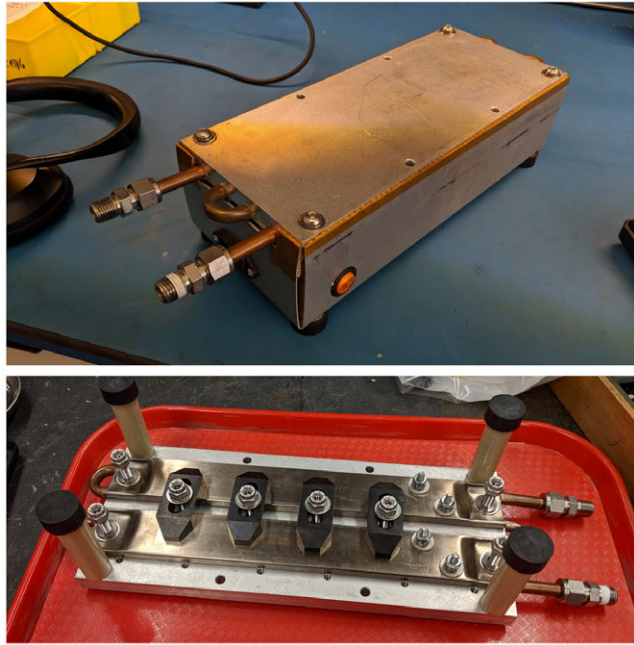
Figure 4-6: Custom build liquid-cooled hot plate for rapid cool down after soldering battery cells.

Each sample consisted of an 18650 battery cell and square piece of MCPCB placed on a hot plate, sandwiching a small amount of 57Bi/42Sn/0.4Ag solder paste solder paste between. Samples were exposed to the same heating profile, starting from room temperature – heat until the cell surface near the bottom reaches $100°C$ or exceeds $80°C$ for more than 30 seconds, then rapidly cooled by turning off the heaters and pumping water through the cold plate from a room temperature reservoir. This setup is capable of cooling samples $from 100°C$ to ambient in less than 30 seconds, reducing the thermal soak time of the battery to prevent insulator breakdown. The process is monitored via handheld thermocouple reader with the top surface of the hot plate and one cell instrumented near the base to avoid overheating.

4.3.2 Solder Sample Testing

After cooling to room temperature, the samples are gripped by the corner of the MCPCB with pliers and the cells are removed by applying a bending load to the cell by hand until the solder joints fail. Microscope viewing of the solder joint reveals porosity and wetting of the surfaces in addition to any visible peeling of the copper foil from the MCPCB that indicates a strong joint has formed. Fixtures were conducted to break solder joints with an Instron to measure stiffness and strength, but ultimately were not able to be used before the conclusion of this research.
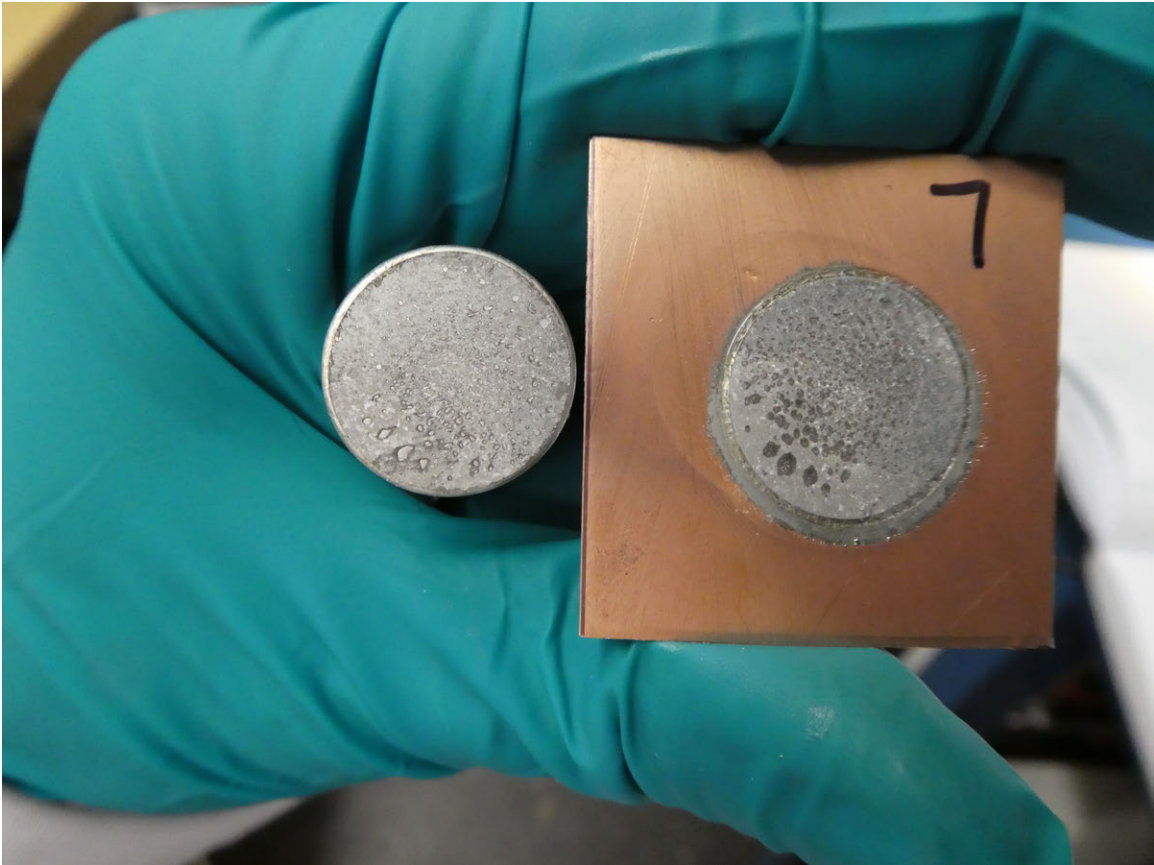

Figure 4-7: A soldered cell sample torn from the MCPCB to inspect the solder joint. There is visible porosity despite the moderately strong bond.

4.3.3   Electroplating

Electroplating offers another avenue for improving solder joint quality. Electronic components designed for soldering are often plated in tin solder (HASL) or gold (ENIG) to maximize solder joint quality. The plating layers prevents underlying metals such as copper from oxidizing over time, losing the ability to form solid solder joints without contaminants and wetting poorly. Gold and tin plating readily wet with most solder alloys and resist corrosion and oxidation to provide a long shelf life. Further, almost all common solder alloys contain tin and the common metal content on the bond surface greatly expedites bond formation and improves bond strength in a solder joint.

Pertaining to soldering battery cells to MCPCB's, the steel can of an 18650 is nickel plated for corrosion protection but has the side effect of being a relatively poor metal for direct soldering. Combined with the high heat capacity of the battery can and conductivity into the jelly roll, it can be quite difficult to heat the nickel surface high enough to directly solder to the cell in a timely manner. Since the solder alloy of choice is 42 percent tin, a tin plating is highly desirable to improve wetting and rapid formation of intermetallics. Plating the array of disconnected copper pads etched on the MCPCB is easily accomplished with the same electroless tin process used in PCB production and purchasable from a plating supplier such as Transene. The Bright Electroless Tin kit provided by Transene utilizes an acidic solution that does attack aluminum, so the aluminum surfaces were completely covered with chemical resistant polyester plastic powdercoat masking tape to prevent exposure to the bath. Following Transene's preparation guide, the MCPCBs were immersed in the plating bath for 10 minutes at $85°C$ to produce a 65 micro-inch tin plating.

The nickel surface of the battery cells cannot directly accept a tin plating, but is readily electroplated with copper which can be followed by tin plating (or electroless). Further, electroless platings generally require high bath temperatures to maintain dissolved metal ions, and the typical range of $80 - 90°C$ for 10 minutes of plating time is unacceptable for a battery cell. Electroplating tin and copper can both be
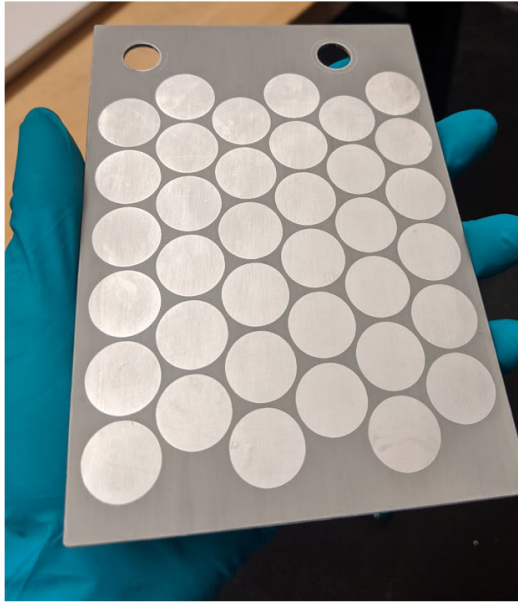
Figure 4-8: Electroless nickel plating results on copper pads of etched MCPCB.

done at room temperature, which is much more desirable and still reasonably fast to do because only the small planar bottom surface of each cell needs plating. A copper sulfate plating bath was prepared by dissolving ZEP Root Kill in hot water at a concentration of 400 g/L. Using a copper plate electrode and a lab power supply, cleaned and degreased cells were plated for 5 minutes at a constant current of 70 mA using a lab power supply, which empirically produced a consistently bright copper finish that is well bonded to the cell. A sample of cells were then additionally tin plated in a stannic chloride bath produced by dissolving tin metal in 20 percent HCL solution until saturation and using a pure tin electrode at the same current density and plating time.

Tin, copper, and unplated cells were firstly evaluated side by side using a Hakko FX100 soldering iron with a 5mm wide chisel tip and flux-core Sn63Pb37 solder wire. Cells were fixed vertically and the iron set to boost mode for maximum heat output. With a freshly cleaned and tinned tip, the side of the iron was applied in full contact to the center of the cell bottom and observed for speed and quality of the molten solder to wet the cell surface. There was a significant and noticeable speed improvement with the copper and tin plating vs the unplated cell, with no noticeable difference
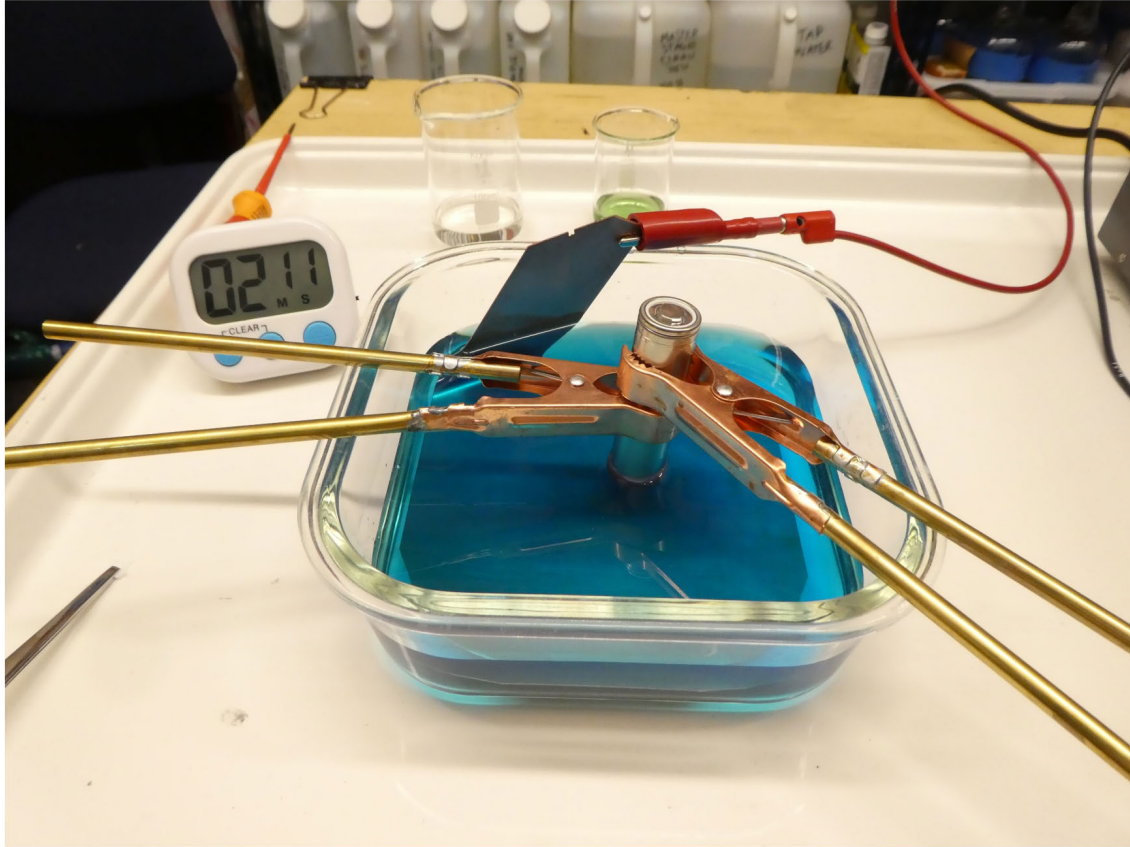
Figure 4-9: Simple copper plating bath setup for a single cell.

with the tin vs copper plating.

A secondary set of tests was conducted by again soldering single-cell samples to small squares of MCPCB and manually tearing the cells from the substrate after the soldering process was complete. In this set of tests, direct comparison between unplated, copper, plated, and copper-tin plated cells showed improved bond strength with the plated cells under identical solder volumes and reflow conditions. In some samples the solder bond exceeded the peel strength of the copper foil in some areas, tearing it off the polymer ceramic below.

4.4   Cold Plate Fabrication

The cold plate base is machined from 3/8 inch thick MIC6 aluminum tooling plate to maintain flatness and eliminate any warping from internal stress after machining,
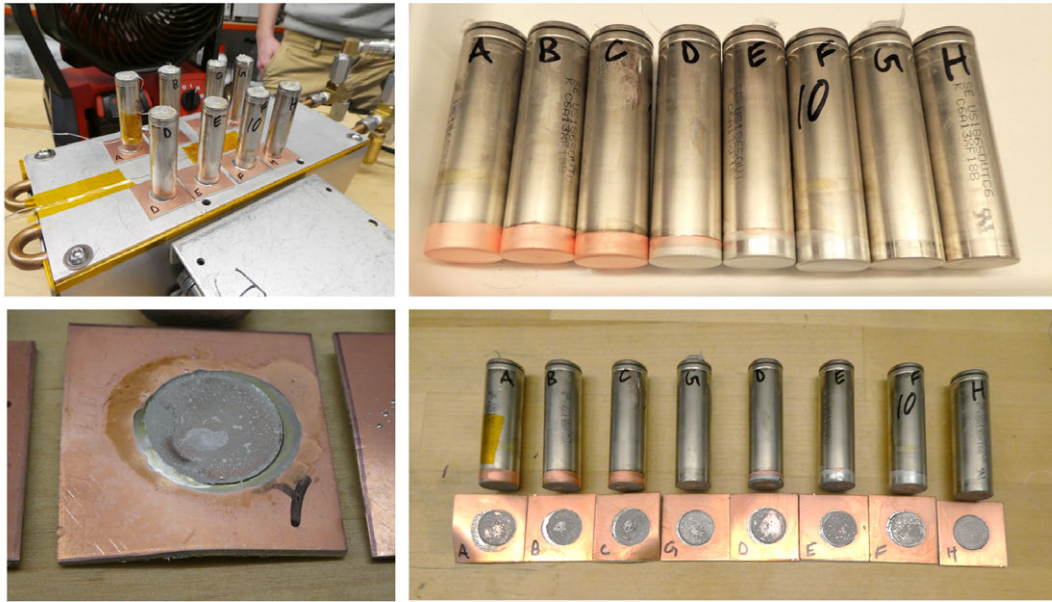
Figure 4-10: Electroplated cells and test results from tearing. There is visible peeling of the copper from the polymer layer on the MCPCB, indicating improved bond strength.

critical to ensure the dovetail joints mate freely. Stock plates were prepared by an initial operation to mill four holes counterbored for low profile socket head cap screws. The plates were then bolted onto a fixture plate held in a vise to allow full five sided CNC machining of the base plate channels and dovetails in a single operation. After machining, all parts were carefully deburring with a scraper, files, and rotary tool followed by a thorough cleaning and degreasing.

4.4.1 Leak Testing

To validate the pressure holding capability of the dovetail and silicone adhesive attachment design, a sample was prepared with a 1/16" aluminum sheet in place of the MCPCB. After thoroughly cleaning both parts in an ultrasonic cleaner with mild degreaser, Loctite Red silicone RTV was dispensed with a syringe on the base plate grooves and dovetails. The silicone acted as a lubricant for sliding the top sheet on the dovetails and into position, enclosing the fluid cavity fully. The ends of the dovetail
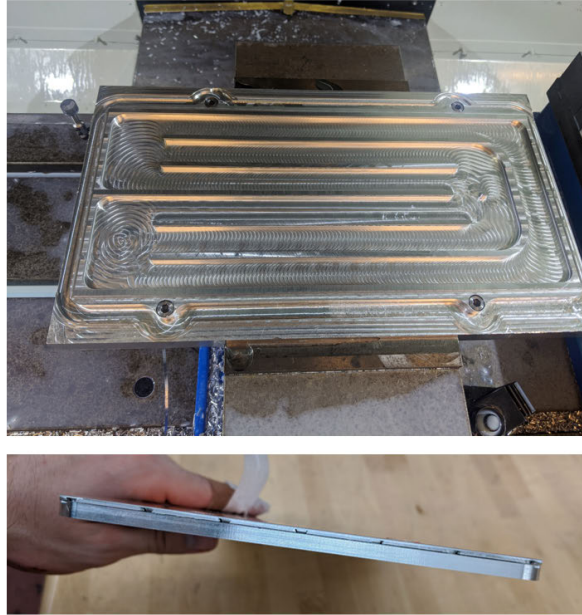
Figure 4-11: Machining and assembly of the cold plate with a good fit of the dovetails.

grooves were then carefully filled with more silicone RTV and allowed to cure for 24 hours. After curing, the test article was fitted with fittings and connected to a 827 kPa (120 psi) air line through a pressure regulator manifold. Immersed in water, the air pressure inside the cold plate was slowly increased in 34 kPa (5 psi) increments and held for 2 minutes until failure at 414 kPa (60 psi).

Figure 4-12: Assembled pressure test article with silicone RTV adhesive. Pressurizing with air caused silicone to burst a small pinhole at 414 kPa (60 psi), visible at right.

5

Thermal Testing

To confirm the viability of the initial concept for axial end cooling 18650 cells soldered to MCPCB material, a single cell test article was constructed, instrumented, and discharge tested in a custom single cell test bench.
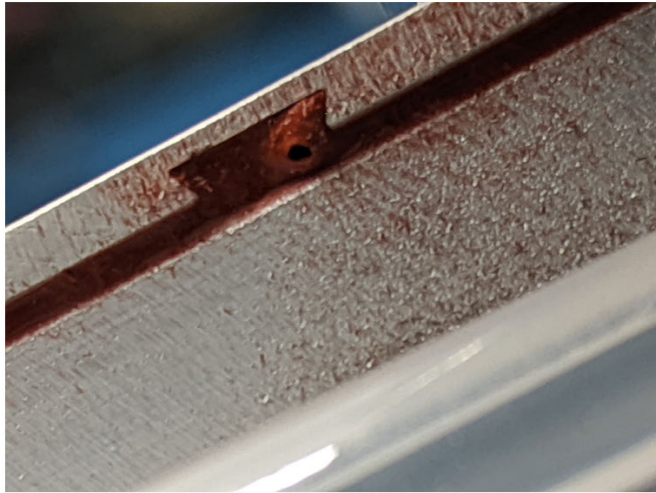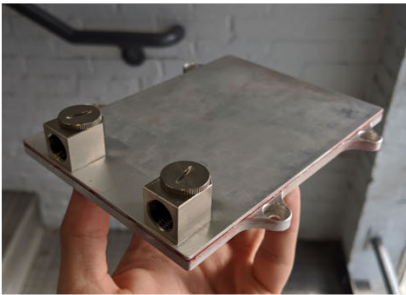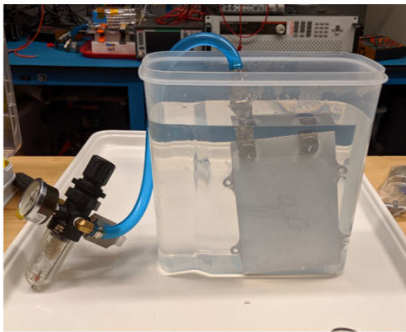
5.1 Test Article Preparation

A new Sony VTC6 cell was removed from heat shrink sleeve and ultrasonically cleaned and soldered to a 30 mm square of Polytronics TCB-C MCPCB material, with 1.5 mm thick aluminum substrate and 2 oz copper foil. The MCPCB was placed on a laboratory hot plate with a small amount of Chip Quik solder paste, composition Sn42/Bi57.6/Ag0.4 in T4 mesh size with synthetic no-clean flux. The cell was placed on top and gently pushed down until the solder paste was just visible at the perimeter of the cell. The solder paste was chosen for inexpensive commercial availability and low melting point of $138°C$. The cell and MCPCB were both instrumented with a type K thermocouple as close as possible to the solder joint. The temperature of the cell and MCPCB surface were monitored with a handheld thermocouple reader.

The hot plate is turned on to maximum heat and the cell temperatures monitored until the cell reached $80°C$, at which point a timer was started After 30 seconds the cell surface approached $100°C$ and the solder had flowed to produce a shiny solder joint and fillet around the entire cell. At this point the hot plate was turned off

and the MCPCB carefully moved to a room temperature aluminum plate for rapid cooling. The total duration of the cell surface exceeding $80°C$ was less than 60 seconds. After cooling, the solder joint was carefully inspected for visual joint quality under magnification. The MCPCB was then trimmed to a roughly 30 mm circle with a bench shear. The MCPCB was turned round to a diameter of 22 mm by using a metal lathe clamping the assembly by the cell in a 23/32 inch collet to ensure concentricity with the cell axis.

5.2 Test Setup

The test setup is designed to clamp the MCPCB from the perimeter with a inch Swagelok tee fitting such that isothermal cooling water can flow across the bottom surface and cool the cell via conduction through the solder joint. The steep taper of the Swagelok fitting receptacle forms a knife edge that creates a water-tight seal when deformed into the MCPCB by sufficiently tightening the B-nut. A stainless steel tube running through the tee fitting focuses the water on the center of the cell, returning through the annular cavity around the tube out the branch of the tee fitting to return to the tank. A small pump provides a continuous circulation of water from a one-gallon reservoir constructed from a beverage dispenser. The cell is electrically connected to a power supply and electronic load via a custom designed PCB that clamps to the top of the cell with a shaft collar and uses an array of spring loaded contacts to adapt the terminals of the cell to a set of screw terminals. The PCB includes sense contacts on separate spring contacts to avoid voltage drop from the high current path from affecting measurements. The cell and PCB are thermally insulated from natural convection with several layers of aluminized mylar bubble wrap insulation.

5.2.1 Instrumentation

The test setup is instrumented with seven type K thermocouples along the length of the cell and an eighth thermocouple measuring the inlet water temperature. An
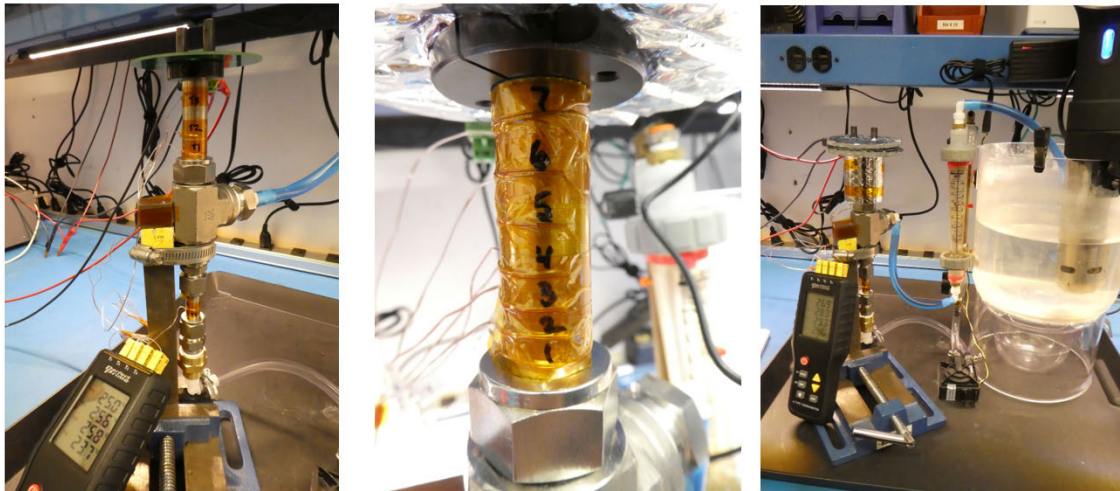
Figure 5-1: Single cell set up in the endcooling test bench with 7 type K thermocouples from top to bottom.

analog float flowmeter is used to observe the flow rate of the system. The cell terminals are connected to a Tektronix 2380-120-60 electronic load and a Tektronix 2280S-32-6 precision power supply for charge and discharge cycling. A Tektronix DAQ6510 data acquisition system with 7708 multiplexer card was used to record all thermocouple temperatures, monitor the cell voltage, and monitor discharge current utilizing the current monitor output of the electronic load. All data was recorded at 1 hz. [4][5][6]

5.2.2 Test Procedures

After clamping the cell sample properly in the test setup and installing thermal insulation, the pump is turned on to purge air from the system and allow the cell to thermally stabilize to the room temperature water reservoir over the course of 30 minutes. The test setup relies on the large thermal mass of the water to sink the heat from the cell with negligible temperature rise, providing an effectively isothermal coolant temperature to the cell throughout discharge testing. The cell is CC-CV charged with the power supply to 4.20 V with a 6 A current limit until C/40 cutoff at 75 mA. After 2 minutes to allow the open circuit voltage to stabilize, the cell is discharged under CP load until cutoff at 2.50 V. Discharge tests were conducted at 34.73 W, 46.30 W, and 60W representing vehicle-level power consumptions of 30 kW,

40 kW, and 52 kW respectively based on an 864-cell pack size utilized by MY19.

5.3   Limitations

The temperature profiles from the single cell test shows several limitations. Firstly, the electrical connection method with the custom PCB utilizing spring contacts and shaft collar is not representative of the intended RSW connections to thin nickel foils and fuse elements. The large steel shaft collar and PCB assembly at the top of the cell offer considerable thermal mass that is sinking heat from the cell and cooling it by conduction. This is visible in the data by observing that the top of the cell is actually cooler than thermocouples closer to the middle. The electrical connection resistance of the spring contacts is likely higher than RSWs, estimated to be 1-2 mOhm per the manufacturer's datasheet, which would contribute a not insignificant amount of heat. Contrarily, the nickel foil with fuse element also has a different resistance and joule heating in the bus bar would couple back into the cell. The two setups deviate in the additional thermal mass available in the test setup, whereas the actual implementation in a spot welded array would likely cause the cell to be heated by the bus bars instead of the other way around. Additionally, the focused jet of water aimed at the cell is not representative of the parallel water flow implemented by a low profile cold plate design, but instead represents a best case scenario where heat transfer is maximized with the water.

6

Results and Conclusions

The goal of this project was to investigate the viability of a novel concept for a liquid cooled battery pack used in a Formula SAE Electric vehicle. The development process explored areas of manufacturability, thermal performance, and fluid performance. From a manufacturing standpoint, the two areas of development were in cold plate construction and cell attachment. Thermal performance was evaluated at the single cell scale and fluid performance was tested with pressure and flow rate testing to failure.

6.1   Cell Bonding

Incremental prototypes and comparative testing evaluated several attachment methods for bonding the cells to the cold plate including cold welding and soldering with various fluxes, alloys, and surface treatments. Cold welding with indium alloys was ultimately ruled out due to inherent structural compliance in the cell bottom that is not suitable for the cold welding process. Soldering in contrast showed great capability to rapidly bond a large array of cells utilizing a specialized hot plate that can rapidly cool the solder joints to avoid damaging the cells with prolonged heating. Chosen for the lower cost and scalability with comparable bond strength and quality, the solder paste process showed noticeable wetting and bond strength improvement when paired with copper and tin plated cells. The limitations of this

testing are purely qualitative without a larger number of test samples and repeatable instrumented fixturing for pull tests, but differences in porosity and peeling of the copper foil of the MCPCB are good indicators of improvements in joint strength. From a manufacturability standpoint, all processes used to produce the cell to cell bond to the MCPCB are inexpensive, widely accessible, and scale well to large quantities and module sizes – CNC machining the MCPCB, etching the cell grid pattern into the copper foil with a vinyl-cut mask, tin/copper plating, and solder paste dispensing.

6.2 Thermal Test

The recorded data from each of the cell discharge tests show the cell voltage, current, heat generation, and surface temperature rise over time starting from 25 C ambient conditions. With a critical surface temperature of 80 C per the manufacturer's recommendation and 60 C per FSAE rules, the tests conducted show that the cooling design is viable to support an FSAE vehicle. At 34.73 W, the cell maximum temperature rise measured was $26.0°C$ with the coolest $16.0°C$, representing a $10°C$ gradient across the cell. At 46.30 W this jumps to $35°C$ and $21.5°C$ respectively with $13.5°C$ delta, and 60 W constant power discharge levels result in a $46.5°C$ maximum and $28°C$ minimum for a $18.5°C$ temperature difference between hottest and coolest. Considering the 34.73 W per cell represents an RMS vehicle power of 30 kW using MY19's cell count of 864 and this is higher than empirical race data from the endurance event, this design could support a vehicle similar to MY19 at a 30 kW RMS power without hitting the $60°C$ thermal limit in ambient conditions as high as $34°C$ if temperatures were sensed at the hottest part of the cell. If ambient conditions are lower, then much higher power levels up to 50 kW or more could be supported on a cool day. This single cell test does demonstrate viability, but there are some critical differences in the setup vs in a pack that are affecting the test data. The ideal inlet condition of the water being isothermal and at ambient temperature assumes a perfectly efficient radiator system in the vehicle capable of rejecting all the heat to ambient, which is impossible to obtain. It would be more appropriate to expect a
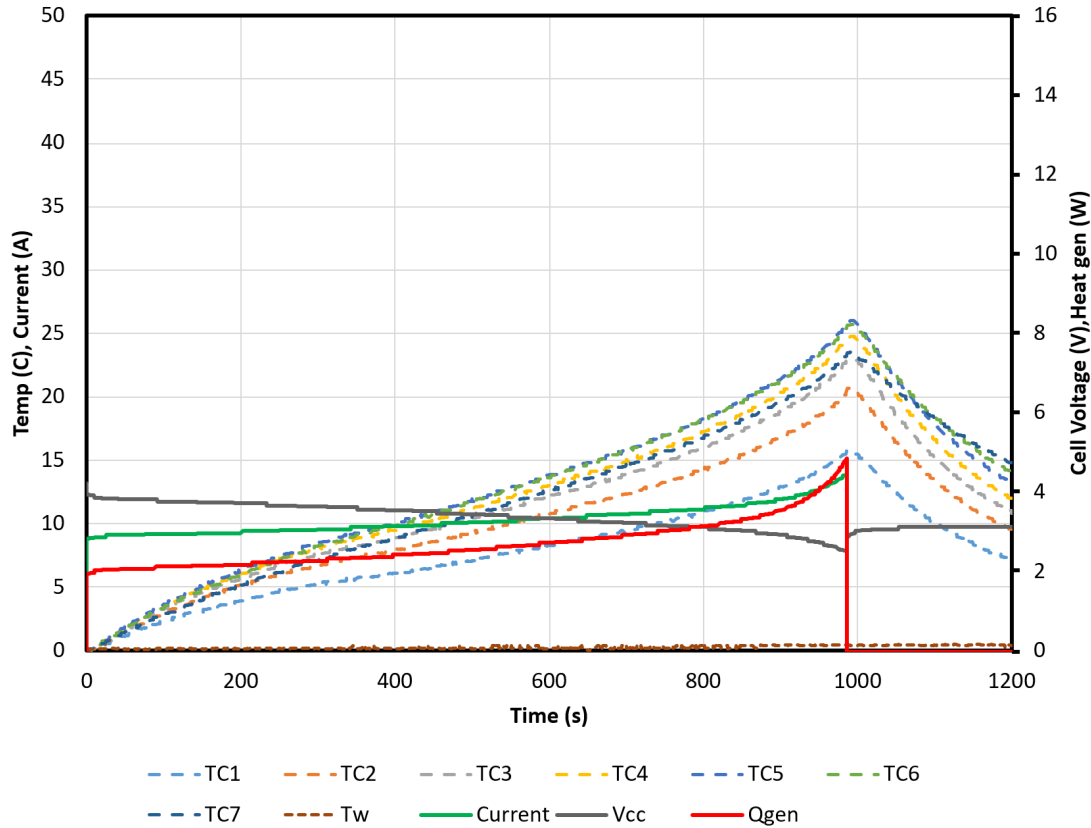
Figure 6-1: Single cell endcooling at discharge of 34.73 W continuous.

water inlet temperature $5-8°C$ hotter than ambient conditions if not more, which would linearly increase the cell temperature by the same amount. Additionally, the top of the cell in a real pack would not be heatsunk by shaft collar and PCB in the experiment, so it would also rise to a hotter temperature. Practically speaking, there is an important loophole in the FSAE rules that allows temperature sensing anywhere within 10 mm of the negative terminal, and since the can of the cell is the negative terminal, you could place the thermistor closer and closer to the cold plate to measure cooler temperature without technically breaking the rules even though the top of the cell could easily exceed $60°C$. There's further nothing preventing you from placing the temperature sensors directly on the cold plate, where they would only effectively report the coolant temperature on the other side! In the spirit of battery cell safety, however, the top to bottom temperature gradient should be taken into account to
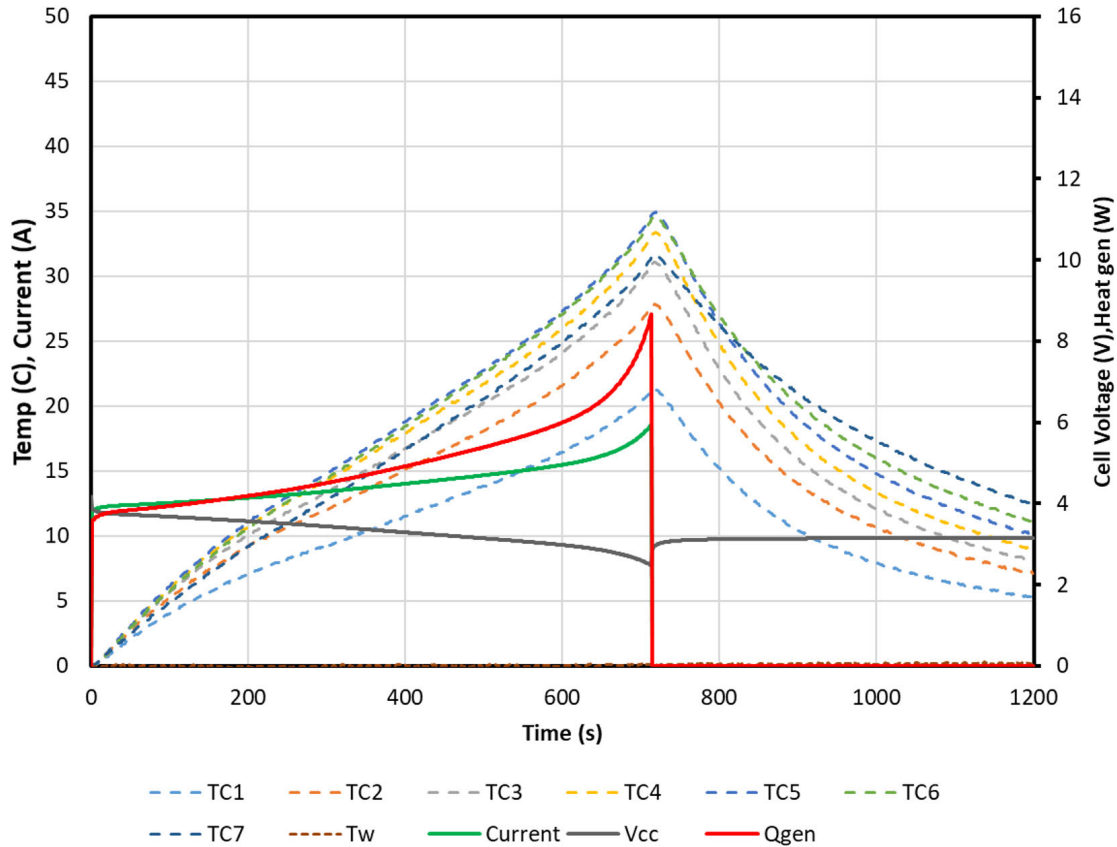
Figure 6-2: Single cell endcooling at discharge of 46.30 W continuous.

ensure the hottest part of the cell never exceeds $80°C$.

6.3   Cold Plate Performance

Regarding fluid performance, the pressure silicone seal failure at 414 kPa (60 psi) vastly exceeds reasonable pressures in an FSAE coolant system which are in the range of 103-138 kPa (15-20 psi) based on measured pressures in the MY19 battery pack. Though full size cold plates were never tested for pressure drop flow rate curves and leak pressure, based on similarity to MY19 battery cold plates a 7-14 kPa (1-2 psi) pressure drop is expected in the range of 4-8 LPM, which would ballpark the maximum system pressure around 103-138 kPa (15-20 psi) for a six module series loop. The failure mode of the cold plate to fail by blowing out the silicone instead of breaking and peeling open at the adhesive joint is also a distinct improvement over MY19,
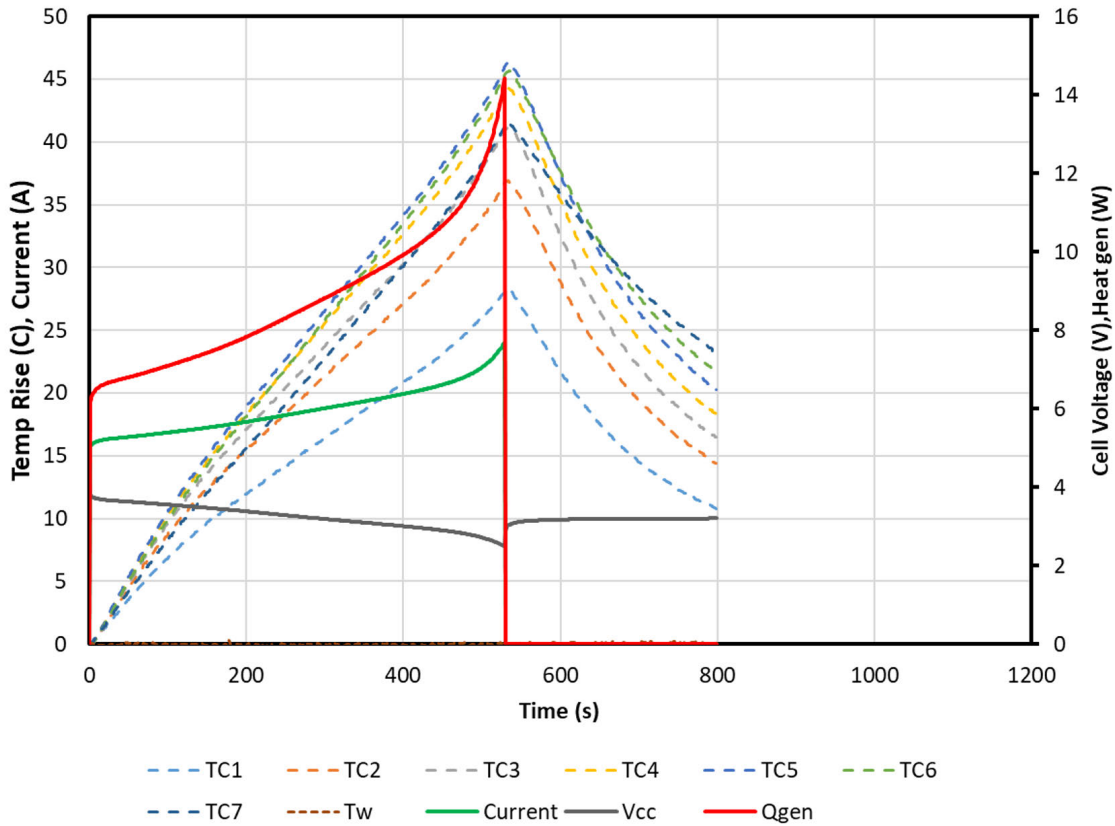
Figure 6-3: Single cell endcooling at discharge of 60.0 W continuous.

where the modules could inflate and separate the epoxy seal joints if overpressurized beyond 207 kPa (30 psi). The metal interlocking dovetail joints and compression loaded silicone RTV prevents any separation from happening until the aluminum itself fails, which is long after the RTV will blow out and relieve the pressure. The overall design produces a cold plate that is only 7.8 mm thick in total height with a mass of 0.69 kg per 144 cell module, maximizing module power density and pushing energy density to near 0.72 MJ/kg (200 Wh/kg).

7

Future Work

The work presented in this thesis is only the very start to proving out and progressing the proposed design into a viable battery module prototype. Ongoing and future work was ultimately ended by the unexpected onset of the COVID-19 global health pandemic which prevented build of larger modules, further cell property testing, and cell bond quality measurements.

7.1   Soldering

Further process development remains in refining the soldering process to determine optimal solder dispensing volume, dispensing pattern, and reflow temperature profile to minimize voiding with quantitative results. Fixturing single cell samples into an Instron fixture to allow repeatable joint failure measurements is also critical to understand how stiff and strong the solder joints are, and if there are any causes for concern with vehicle loads presented from driving and crash scenarios. Low voiding is also critical to improving the thermal conductivity between the cell and MCPCB material, though it is noted that even with the considerable voiding present in the single-cell test articles the cell could be adequately cooled. Decreased voiding therefore stands to only improve the viability of the MCPCB end cooling concelpt. Other surface treatments such as different active fluxes and plasma treatment of the surfaces before soldering could further aid the adhesion of the molten solder to the plated

substrates and reduce voiding.

7.2 Electroplating and MCPCB Fabrication

The tin and copper plating treatments require some optimization to obtain the strongest possible bond between substrate and plating, there are some issues with the nickel coating on the cells only weakly adhering to the copper plating. In scaling to a production process, this process would ideally be run by an external plating house with specific expertise and specialized tooling to allow plating battery cells without damage. The MCPCB component is fully within the manufacturing capabilities of production PCB houses, which could easily produce the fully plated sheet from raw MCPCB stock with typical design files. The only post-machining required would be the large G1/4 threads for fittings and the dovetail grooves, which are beyond the scope of typical PCB production facilities. Outsourcing the bulk of manufacturing on the MCPCB would also improve product consistency and benefit from volume scaling to reduce price.

7.3 Prototype Modules

Work should also continue in building larger scale prototypes up 36 cells and a full 144-cell module, which will be the true validation tests once run at full power on battery cycling equipment. Scaling up the module size will inform the scaling of manufacturing and reveal any problems caused by mass-soldering of many cells at once or any CTE/deformation issues caused by the soldering process. Operating larger modules also informs module-scale thermal deviations such as hot spots near bus bars, current imbalance, thermal gradients across the pack, and water temperature rise within a module moving heat between the cells that will all diminish performance of the overall module versus single cell evaluations. Tooling and parts to build 36-cell modules and a 144-cell module were constructed, but neither prototypes could be completed before the end of research.

7.4 Potting and Compliance

Practically speaking, the cell array is quite dangerous with exposed can side walls in close proximity. Additionally, filling the interstitial volume between cells with a potting compound of some type is desirable to provide thermal mass and heat transfer to even out cell temperature gradients, but there is a tradeoff with module rigidity and weight. Also, the asymmetric nature of the jelly-roll internal construction causes cylindrical cells to deform and expand/contract as they change temperature and charge and discharge. This very small movement on a per cell basis can cause very large movements in a module-size array, and could have dangerous implications for cracking potting compounds or breaking solder joints of compliance is not maintained in the correct locations. Further investigation into the mechanical properties, stiffness, and compliance of the structure will be important to understand how well it will survive in a racecar application.

Bibliography

[1] SAE International. About formula sae series, [online]. available: https://www.sae.org/attend/student-events/formula-sae-electric/about. [accessed:15-may-2019], 2019.

[2] LLC Polytronics Tech. Tcb-c, [online]. available: https://polytronicstech.com/tcb-c/. [accessed:15-may-2019], 2019.

[3] J.K. Ostanek S.P. Miller J.M. Heinzel A. Jain S.J. Drake, D.A. Wetz. Measurement of anisotropic thermophysical properties of cylindrical li-ion cells, 2013.

[4] Tektronix. Daq6510 data acquisition and logging, multimeter system, [online]. available: https://www.tek.com/keithley-switching-and-data-acquisition-systems/keithley-daq6510. [accessed:15-may-2019], 2019.

[5] Tektronix. Keithley 2280s series, [online]. available: https://www.tek.com/tektronix-and-keithley-dc-power-supplies/keithley-2280s-series [accessed:15-may-2019], 2019.

[6] Tektronix. Series 2380 dc electronics load, [online]. available: https://www.tek.com/dc-electronic-load/series-2380/. [accessed:15-may-2019], 2019.